DEPARTMENT OF DEFENCE

DEFENCE SCIENCE AND TECHNOLOGY ORGANISATION

R.A.N. RESEARCH LABORATORY

EDGECLIFF, N.S.W.

INTERNAL TECHNICAL MEMORANDUM 3/80

HEAT CAPACITY MAPPING MISSION
PROJECT HCM-051
PROGRESS REPORT TO 30 APRIL 1980

by

C.S. NILSSON, J.C. ANDREWS, M.W. LAWRENCE,

S. BALL and A.R. LATHAM

INTERIM REPORT ONLY

MAY 1980

DEPARTMENT OF DEFENCE

RAN RESEARCH LABORATORY

INTERNAL TECHNICAL MEMORANDUM 3/80

HEAT CAPACITY MAPPING MISSION
PROJECT HCM-051
PROGRESS REPORT TO 30 APR 1980

C.S. NILSSON, J.C. ANDREWS[1], M.W. LAWRENCE, S. BALL[2], and A.R. LATHAM

ABSTRACT

This report covers progress on NASA Project HCM-051 to 30 Apr 1980. Ground truth data have been gathered to compare to HCM Infra-red images and these data are analysed to delineate the Tasman Front. The status of IR photographic image and computer-compatible tape (CCT) processing is presented and an example of an enhanced image is presented.

POSTAL ADDRESS: The Superintendent, RAN Research Laboratory
P.O. Box 706, Darlinghurst N.S.W. 2010

1. Present address: AUSTRALIAN INSTITUTE OF MARINE SCIENCE, TOWNSVILLE, QLD.
2. Marine Physics Group, WSRL, DEFENCE RESEARCH CENTRE, SALISBURY, S.A.

CONTENTS PAGE NO.

1.	AIMS OF HCM-051	1
2.	GROUND-TRUTH DATA	1
3.	OBSERVATIONS OF THE TASMAN FRONT	2
	3.1 Introduction	2
	3.2 The experiments and data analysis	3
	3.3 Dynamic topographics, currents and transports	5
	3.4 Water column integrities and thermocline shapes	7
	3.5 Meanders and isolated eddies	9
	3.6 Surface temperature	13
	3.7 Some satellite observations	17
	3.8 Scales of the motion and linearity	20
	3.9 Discussion	23
4.	STATUS OF HCM-051 IMAGE PROCESSING	28
	4.1 Photographic image processing	28
	4.2 Computer-compatible tape (CCT) processing	28
5.	AN ENHANCED IR IMAGE 21 AUG 1978	30
6.	COMPARISON OF IR IMAGE AND GROUND-TRUTH DATA	31
7.	THE NEED FOR SYNOPTIC (IR) DATA	32
8.	PRIORITIES OF HCM DATA PROCESSING AND JUSTIFICATION OF DATA NEEDS	33
9.	PUBLICATIONS	34
10.	ACKNOWLEDGEMENTS	34
11.	APPENDIX: STATUS OF CCT PROCESSING (02 APR 80)	35
12.	REFERENCES	45

1. AIMS OF HCM-051

The primary aim of this experiment is to relate the surface infra-red manifestations of the East Australian Current (EAC) and the Tasman Front (as seen by satellite) to the subsurface associated variability of temperature and salinity (as measured from ships and aircraft). Where this can be done, the sea surface temperature images obtained from HCM-051 will be used to obtain time series pictures of the EAC area in order to study the behaviour of the EAC and the Tasman Front.

A secondary aim is to study oceanographic fronts and eddies over the whole area covered by HCM-051, in particular to study the temporal and spatial variations of the Sub-Tropical Convergence south of Australia.

2. GROUND TRUTH DATA

Oceanographic surveys by ship in the Tasman Sea in support of HCM-051 were undertaken by the Australian Defence Science and Technology Organisation as follows:

DATE	AREA	HCM DAY NOS.
27 Jul - 4 Aug 78	Sydney - Sydney	092 - 100
4 - 11 Sept 78	Sydney - New Zealand	131 - 138
11 - 16 Feb 79	Sydney - Brisbane	291 - 296
22 Feb - 1 Mar 79	Eden - Sydney	302 - 309
25 Feb - 1 Mar 79	Brisbane - Sydney	305 - 309
8 - 13 Mar 79	Sydney - Eden	316 - 321

Oceanographic surveys by Royal Australian Air Force Orion aircraft in direct support of HCM-051 using air expendable bathythermographs (AXBT) probes were completed as follows:

DATE	LATITUDE	HCM DAY NOS.
29 - 30 Aug 78	30 - 35^{o}S	125 - 126
13 Dec 78	30 - 35^{o}S	231
8 Feb 79	28 - 33^{o}S	288

Much of these data are yet unpublished. However, the data pertaining to the Tasman Front have been largely analysed and written up for publication. This analysis is given in the next section.

3. OBSERVATIONS OF THE TASMAN FRONT

3.1. Introduction

The question of what happens to the East Australian Current after continental separation has been addressed by several authors beginning with Wyrtki (1962) who postulated that a broad zonal flow of about 500km width was fed by the East Australian Current and crossed the Tasman Sea at latitude 35°S. More recently Stanton(1975,1976) and Denham and Crook (1976) have studied a narrow meandering zonal current frequently found between North Island of New Zealand and Norfolk Island. This current is structurally similar to the East Australian Current, though much weaker, and this leads both Stanton and Denham and Crook to support Warren's (1970) contention that a zonal jet is the most theoretically plausible current system across the Tasman.

The evidence for such a current has been collected mainly, close to the Australian and New Zealand mainlands, with very little data taken more than 300 miles beyond the continental shelves. The central Tasman Sea has been neglected largely because of the limited endurance of the research ships involved; there have been several cruises which crossed the Tasman but no extensive grid searches were conducted in the central Tasman.

In this section we discuss the results of large scale surveys using ships and aircraft near latitudes where the zonal jet should exist. The surveys extended mid way across the Tasman Sea and in one case as far as New Zealand. Broadly speaking, the main result is that the conjunction of the warm water from the South-Coral Sea and the cold water from the Tasman Sea is seen as a very abrupt thermal front at all depths. The associated pressure gradient gives rise to very swift currents along the Tasman Front towards New Zealand. Gross meridional distortions of the

Front occur as water of South-Coral or Tasman Sea origin breaks through the Front to form respectively warm core eddies in the Tasman Sea or cold core eddies in the South-Coral Sea.

3.2. The experiments and data analysis.

A Royal Australian Air Force Orion aircraft deployed air expendable bathythermograph (AXBT) probes at the positions shown by the filled circles on Fig. 1a on 29 August 1978. A course for HMAS Diamantina was then chosen to investigate features revealed by the AXBT survey. This track (4-11 September 1978) is shown as the dashed line on Fig. 1a. Expendable bathythermograph (XBT) probes were released at intervals of about 20km and surface water was continuously sampled with a thermosalinograph. The open circles on Fig. 1a show positions where XBT probes were released from HMAS Diamantina during 13-18 September to extend the earlier coverage.

No ships were used during the second experiment (13 December 1979) when a RAAF Orion deployed AXBT probes at the positions shown by the filled circles on Fig. 1b.

Fig. 1c represents the third experiment. The dashed line shows the track of HMAS Kimbla (11-19 February 1979) where a geomagnetic electrokinetograph (GEK) was used to obtain ocean current vectors at intervals of about 30km, interleaved with similarly spaced XBT's and in conjunction with continuous surface thermograph data. This track was chosen to investigate features revealed by AXBT's deployed at the positions marked by filled circles on Fig. 1c from a RAAF Orion on 8 February 1979.

The fourth and final experiment was a ship survey (HMAS Diamantina, 22 February-1 March 1979; and 8-12 March 1979) along the tracks shown in

Fig. 1d. A continuous surface thermosalinograph recording was made and XBT probes were released approximately every 20km. Ocean current vector measurements (GEK) were interleaved with XBT measurements.

The standard display for AXBT traces was not used since the resolution is poor; instead a frequency to voltage converter was used with a battery driven strip chart voltmeter in order to expand the temperature scale to 2.0°C cm^{-1}. Dynamic height anomaly (0 re 1300 dbar) was calculated for each bathythermal profile by first calculating the anomaly over the sampled pressure interval from the temperature profile and temperature-salinity curves; secondly a correction for the remaining pressure interval to 1300 dbar was obtained from regression relations between deep temperatures and dynamic height. This method was adopted by one of us (C.S.N) from a suggestion by Godfrey to modify Andrews' (1976) treatment of West Australian Current XBT profiles. The AXBTs measured to 350m while some XBTs measured to 450m and others to 750m. As an example, if $D(z_1/z_2)$ is the dynamic height anomaly over the pressure interval from z_1 to z_2 and $T(z)$ is the temperature at depth z, the relation we used for standard 450m XBTs was

$$D(0/1300) = D(0/450) + 3.71T(450) + 53.15 \text{ (dyn.cm.,°C)}. \quad (1)$$

Contour diagrams of D(0/1300) for the four experiments are shown in Figs. 1a to 1d. Dashed lines are drawn where we consider that even though there are insufficient data, isobars are required to produce a consistent or complete picture. The 190 dyn cm contours in Figs. 1 are heavily drawn to represent the position of the centre of the Tasman Front. This isobar frequently, though not always, coincides with the position of the fastest flowing surface water in the central and western Tasman and South-Coral Seas.

The XBT traces were digitised at integer Celsius values, at flexure points, and at 0, 150, 250 and 450 metres. Some examples of reconstituted XBT profiles are shown in Figs. 2a, b and c but the main displays of vertical structure are vertical isotherm sections to 450m depth as functions of progressive distances along ships' tracks. These were computer generated from the digitised XBT data. Thus Fig. 3a is the section along track BCD of Fig. 1a, Fig. 3b is along EF of Fig. 1a and Fig. 3c is along GHIJKL of Fig. 1c. Surface temperatures obtained from the thermograph traces are plotted above the isotherm sections to allow the eye to correlate surface fronts with deeper baroclinic thermal fronts A complete surface isotherm map obtained from all the thermograph data taken during experiment 4 on HMAS Diamantina is shown in Fig. 4.

3.3. Dynamic topographies, currents and transports.

Figures 1 show that the Tasman Front is a zonal band separating a high pressure region in the north from a low pressure region in the south. The band is created by a collection of cyclonic deformations protruding northward and anticyclonic deformations protruding southward so that the Front takes on more the nature of a planetary wave with a zonal wavevector. In fact Figs. 1b and 1c each contain a full-wavelength with southward currents near the coast and out to sea, connected by a northward return flow. Figure 1d contains one and one half wavelengths along 34°S latitude while Fig. 1a shows two full wavelengths out to 163°E longitude and at least four wavelengths between Australia and North Island. The square on Fig. 1a shows the region where Stanton (1976) found a wavelike meandering zonal jet. It had essentially the same shape and dimensions as the meanders we have drawn between 165°E and North Island. There can be little doubt that the Tasman Front, as its name implies, extends from Australia to New Zealand between the South-Coral Sea and the Tasman Sea. Consideration of thermal structure in the next section shows that the Front is in fact an interface between the cold water of the Tasman Sea and the hot water of the South-Coral Sea.

Geostrophic and GEK currents are quite swift even as far east as Lord Howe Island (159 E). For example the northward branch across 33 and 34°S at 159°E in Fig. 1d had GEK currents up to 1m s^{-1}; near H and J in Fig. 1c the GEK currents were respectively 1.5 and 0.75 m s^{-1} in the directions of the cyclonic isobars. These values are typical of the extreme currents encounted at the Tasman Front. Geostrophic currents calculated from the isobar spacings in Figs. 1 lie in the same range from about 0.5 to 1.5 m s^{-1}.

The following approximate volume transports are based on Andrews (1979) universal velocity profile for the area. This profile allows actual geostrophic velocity profiles to be extrapolated to great depths. He found that actual current profiles attain a vertical asymptote at about 2700 m depth but we will adhere to the historical convention of calculating baroclinic transports over the uppermost 1300 dbar. Accordingly the volume transport, V, is related to the change in dynamic height ΔD(0 re 1300) between two stations by

$$V = 28\times10^{6}\,\Delta D/\sin(\text{latitude}) \quad m^{3}s^{-1}\text{, dyn m.} \qquad (2)$$

At latitudes near Sydney this is about $50\times10^{6}\,m^{3}s^{-1}$ for each metre change in dynamic height.

Applying this analysis to Figs. 1a, b and c we find the southward transport between Coffs Harbour and Sydney has a representative figure of $35\times10^6 m^3 s^{-1}$. This stream then turns eastward and, from Figs. 1a, b and d, we find that the volume flow in the Tasman Front after leaving the continental shelf is about the same. At first glance one might be tempted to say that the Front carries about $35\times10^6 m^3 s^{-1}$ into the central Tasman Sea. In fact, volume transports of beyond $30\times10^6 m^3 s^{-1}$ are associated with eddies adjacent to the Front which recirculate a large fraction of the water and do not allow it to progress continuously eastward. The net eastward transport is estimated from the averaged pressure drop across the band occupied by the Front and its associated eddies. Very roughly, this is about 30cm so the net zonal transport is about $15\times10^6 m^3 s^{-1}$; Stanton (1976) found the transport in the Front within the square on Fig. 1a ranged from 10×10^6 to $14\times10^6 m^3 s^{-1}$.

3.4. Water column integrity and thermocline shapes.

In this section we discuss the difference between the shape of the thermocline in the South-Coral and Tasman Seas generally and in particular we investigate whether the thermocline is modified near the Front.

Figure 2a shows five XBT profiles from the South-Coral Sea, well north of the Front, and five from the Tasman Sea, well south of the Front. The (warm) South-Coral Sea profiles come from leg KL of Fig. 1c near 156°E while the (cold) Tasman Sea profiles come from Fig. 1d along 36°S between 155 and 156°E. We see that the essential difference between the two is that the thermocline is colder at all depths in the Tasman Sea with the maximum difference of about 6°C occurring over about 150 to 300m depth. A slightly more subtle difference enables us to identify the origin of a water column: below the mixed layer, South-Coral Sea profiles are very nearly linear while Tasman Sea profiles have a shallower, rounded, somewhat exponential thermocline down to about 200m where the profile then becomes linear.

The two sets of profiles in Fig. 2a were taken from the same longitude but were about 1000km apart in the north-south direction. Figure 2b contains five warm profiles from near the centre of the anticyclone at 34°S, 158.5°E in Fig. 1d and five cold profiles from near the centre of the cyclonic meander at 34°S, 160°E also in Fig.1d. Thus Fig. 2b contains two classes of profiles only 140km apart (with the nearest from the two classes only 80km apart) and separated by the Tasman Front with the warm water on the South-Coral Sea side and the cool water on the Tasman Sea side. The warm profiles have the linear thermocline characterisitic of the South-Coral Sea while the cool profiles have the shallower rounded thermocline nearer the surface becoming linear beyond 200m depth. Comparison of Figs. 2a and 2b show that the water columns identifiable with either the Tasman or the South-Coral Seas maintain their integrity even in the intense meandering regions near the Tasman Front. There is no significant difference between Figs. 2a and 2b and our experience not only with the data from these experiments but from the many surveys conducted in the west of central Tasman and South-Coral Seas convinces us that the shape and mean temperature of the thermal profile is a valuable indicator of water type and origin in the upper levels in these areas. In fact the Tasman Front is simply a sharp boundary between two bodies of water with different vertical thermal profiles. Currents are driven by the pressure change across the Front and the required feed water comes from the East Australian Current. Hamon (1968a) noticed that a difference in dynamic height implied not only a change in vertically averaged temperature but also a change in thermocline shape although the presence of the Tasman Front was not known at the time.

An obvious question now is "What are the shapes of thermal profiles in warm eddies south of the Front and in cold eddies north of the Front?". We show in section 5 that the low pressure cell in Fig. 1c centred at 32°S, 157.5°E is an isolated cyclonic eddy to the north of the Front; it is obvious from the isobar pattern in Fig. 1d that the anticyclone centred at 36°S, 152°E is isolated and is south of the Front. Figure 2c shows five warm thermal profiles from the centre of the anticyclone and five cool profiles from the centre of the cyclone. Mixed layer temperatures on Fig. 2c are juxtaposed with those on Figs. 2a and b, an event which could have many causes. The important point is that the warm eddy has the linear thermocline typical of South-Coral Sea water and the cool eddy has the shallow, rounded thermocline typical of the Tasman Sea. There has been some cooling of the thermocline in the warm eddy and some warming of the thermocline in the cool eddy, of about 1°C over the interval 100-450m. This is presumably due to lateral, small scale eddy diffusion of heat into the cold eddy embedded in the warm South-Coral Sea and out of the warm eddy embedded in the cold Tasman Sea. We conclude that when eddies detach from meanders of the Front, the thermoclines in the centres of the eddies largely maintain their integrity.

3.5. Meanders and isolated eddies.

It is obvious from Figs. 1 that the position of the Tasman Front varies markedly in space and time by executing mesoscale, lateral meanders. These give the Front an appearance similar to the Gulf Stream after it turns eastward to form an interface separating "slope water" from Sargasso Sea water; it is also quite like the Kuroshio-Oyashio front.

We now address the question of which of the meanders in Figs. 1 can properly be called closed eddies and which of the closed eddies can properly be regarded as detached from the main frontal system. The criterion we adopt for calling an eddy closed is that surrounding some central pressure anomaly there should be a closed orbit for a circulating water particle. According to this criterion a localised intensification within an elongated meander would be a closed eddy. We regard a closed eddy as detached if its water type is separated from the Sea of its origin (either South-Coral in the case of warm core eddies or Tasman in the case of cold core eddies) by the Tasman Front. Obviously a detached eddy originates in a meander which intensifies into a closed eddy; the final process is the reformation of the Tasman Front behind the break-away entity.

The only data we have for experiment 2 are AXBT profiles and these are summarised in the dynamic topography on Fig. 1b. There is a warm southward meander near the coast and a cool northward meander east of this. As signified by the dashed lines, the sparsity of data at the top of the northward meander prevents any further interpretation of that eddy structure.

Figure 1a provides some good examples of intensifying cyclonic and anticyclonic meanders. Fig. 3a shows the temperature section along the track BCD of Fig. 1a. We have anticyclones located at 32°S, 155°E and at 30.5°S, 160°E on Fig. 1a. The thermal structure of Fig. 3a shows that the first eddy contains anomalously warm surface water (20-21°C) and depressed isotherms in the thermocline between the distance marks of 150 and 500km from B. The fronts are very abrupt at the surface, being only about 30km wide, but are up to 120km wide within the thermocline. The warm surface water (and indeed the whole thermocline) originates in the South-Coral Sea. The second closed anticyclone (near 160°E) is seen as depressed isotherms between the distance marks of 800 and 1030km on Fig. 3a and exhibits a typical anomalously deep and warm winter mixed layer. The 20°C surface water shown at 750-800km on Fig. 3a is South-Coral Sea surface water advected south round the western edge by the eddy current.

There is a cyclonic meander at 30.5°S, 162°E on Fig. 1a which was fairly well delineated by AXBT's (filled circles) partial circumnavigation (cruise track) and a second visit by HMAS Diamantina (open circles). Tasman Sea surface water of about 18°C lay within the meander and the ship's course around DE was chosen in large part by a desire to criss-cross the surface temperature front. This meander contains closed orbits for water particles but intensification, or eddy closure is very poorly developed when compared with, say, the two anticyclones just previously discussed.

We see the next stage of development, namely the beginning of the reformation of the Tasman Front behind a detaching feature, in the cyclonic eddy centred at 30.5°S, 158°E in Fig. 1a. The ship's track crossed this feature centred near the 600km mark on Fig. 3a. This shows the elevation of the isotherms in the thermocline together with the 18°C surface water indicative of Tasman Sea water. There appears to be a swift eastward current south of this eddy along 33°S on Fig. 1a as well as the zonal cyclonic eddy current along 29.5°S. The dynamic height data are too sparse for us to state definitely that the Tasman Front was reforming south of the cyclonic eddy. However surface mixed layer temperatures show anamously warm water drawn out along 33°S to 159.5°E and this reinforces the contoured interpretation we have put on the surface pressure field of Fig. 1a.

The discussion now turns to eddies in the final stage of complete isolation from the Tasman Front. The literature contains many examples of detached anticyclones south of Sydney, adjacent to the Australian coast. Nilsson and Cresswell (in preparation) give a particularly full account of their evolution and even of anticyclone reabsorption by the Tasman Front. Figure 1a shows one such typical high pressure cell near 34.5°S with Fig. 3a showing the vertical structure extending 120km out from B, typical of a winter eddy. Figure 1d shows a typical summer anticyclone south of the Front near 36°S. A trough separates the current ring in the south from the zonal jet in the north and it is worth noting that between 36° and 35°S the baroclinic pressure falls 50cm and then rises 100cm between 35 and 34°S. There is another isolated anticyclone in the south east corner of Fig. 1d. It is elliptical with a major axis parallel to the coastline and a dynamic height relief, from centre to edge, of only 15cm. We know from the shapes of the XBT profiles that it originated from South-Coral Sea water passing through the Front but most of the excess heat has been lost from the thermocline and the central surface temperature anomaly is only slight (see Fig. 4).

The cyclonic eddy shown in Fig. 1c centred on 32°S ,157.5°E has thermal profiles shown in Fig. 2c which identify its origin as the Tasman Sea. Vertical structure in Fig. 3c shows the very strong fronts near the 400 and 750km distance marks and a pool of anomalously cool surface water with a temperature near 24°C within the current loop. The data do not extend sufficiently far in the south east corner of Fig. 1c to show whether the eddy was closed during the air and sea surveys of 8 to 19 February 1979. It was certainly closed and detached by the completion of the ship survey from 22 February to 12 March 1979: the isobar pattern for that survey, Fig. 1d, shows the Tasman Front reconstituted along latitude 34°S, thereby separating the cyclonic eddy to the north from its Sea of origin. The changing position of the Tasman Front can be inferred by considering Figs. 1c and 1d jointly. The most reasonable explanation is that the main current flowed south past Coffs Harbour and Sydney (Fig. 1c), diverted seaward at about 34°S latitude and the northward up 156°E longitude (Fig. 1d) to then flow around an elongated equatorward meander (Fig. 1c) which subsequently pinched off while the main current reformed along 34°S latitude (Fig. 1d).

In summarising this section we may say that eddies apparently are shed to the north and south of the Front as detached meanders. More particularly warm eddies are detached to the south near the coast and one half of a system wavelength further east cold eddies detach to the north. The process may repeat itself with the next sort being warm eddies at one full wavelength, and so on.

3.6. Surface temperature.

In this section the relationship between sea surface temperature and the baroclinic structure of the Front and its eddies is examined, particularly with a view to deciding whether the position of the Front can be monitored remotely (e.g. from satellites). We already know that newly formed winter anticyclones have warm anomalies within their current rings and that both summer and winter anticyclones have tongues of warm northern water advected round the forming eddies (Andrews and

Scully-Power, 1976; Nilsson, Andrews and Scully-Power, 1977; Andrews, 1979). These older data were taken within one half system wavelength of the Australian coast; the present data allow an analysis of cold core cyclones and also warm core anticyclones over a much larger area in both summer and in winter. The winter experimental data from 29 August to 11 September 1978 are shown in Figs. 1a and in Figs. 3a and b. On proceeding north along BC the surface temperature (Fig. 3a) fell from 18 to 17°C. The fall marks the passage into the trough separating the high pressure cell (at B on Fig. 1a) from the Tasman Front to the north. When the Front was crossed near the 150km mark on Fig. 3a the surface temperature rose about 4°C at a maximum rate of 3°C over 6km. The surface temperature north of the Front, within the high pressure cell near C on Fig. 1a, stayed about 3°C higher than the Tasman Sea surface water immediately south of the Front (near B, or 18°C). About 75km along CD (near the 525km mark) the surface temperature fell, just as abruptly as it had risen, back to about 18°C, to mark entry into the almost detached cyclonic eddy. This eddy is marked by the elevated isotherms in Fig. 3a and is bounded to the south by the isobars and the warm mixed layer water extruding along 32.5°S in Fig. 1a. The cool surface water in the cyclonic eddy then merged fairly slowly with a warm peak near the 750km mark on Fig. 3a; the vertical isotherm section shows that the peak, with a temperature near 20°C marks the transition from the cyclone to the anticyclone north east of Lord Howe Island in Fig. 1a. The anticyclone contains surface water about 1°C warmer than that near B. Figure 3a breaks off where the surface temperature fell as the anticyclone's eastern edge was crossed and partial circumnavigation of the cold feature near 162°E on Fig. 1a began.

We have described a sequence of warm and cold patches of surface water associated with cyclonic and anticyclonic eddies near and in the Tasman Front in winter. The story continues across the Tasman Sea with Fig. 3b which has a different sort of thermal signature to Fig. 3a. There is a continual trend of falling surface temperature along EF. The slopes of the isotherms and the coherence of the wavy structure in the thermocline also decline along EF. The data on Fig. 1a in the eastern Tasman Sea are too sparse to allow us to draw many conclusions about the nature of the Tasman Front there, except to say that we think the track EF only cuts across the southern portion of the meander pattern.

One might expect the ocean currents in summer, when surface warming occurs, to be obscured in the sense that the surface temperature signature of deeper baroclinic events might be overlain by surface thermal noise and so be undetectable from ships or satellites. The data from experiments three (8 to 19 February 1979) and four (22 February to 12 March 1979) show that this is not the case and surface temperatures reveal the position of the East Australian Current and the Tasman Front just as clearly in summer as they do in winter.

Surface temperatures are displayed in different fashions for experiments three and four in Figs 3c and 4. Since the data were gathered over a month, Figs. 3c and 4 should not necessarily be expected to match in more than a qualitative fashion. However there is an obvious overall fall of surface temperature from north to south of about 6°C in about 1000km: Near 28°S, on leg KL of Figs. 1c and 3c we have the northernmost data and the highest temperatures near 26°C while the southernmost leg of Fig. 4 has temperatures near 20°C.

The cruise track GHIJKL cuts into the poleward meander on Fig. 3c about 150km from G. The strong front in the thermocline shows the southward baroclinic current which advects hot water from northern latitudes. The surface temperature peaks near the 150km mark at about 26.5°C, so it has obviously been carried south from Brisbane's latitude. This was confirmed by measurements made while HMAS Kimbla returned from Brisbane to Sydney during 24 to 27 February 1979: the GEK showed a current from 3 to 4 knots flowed south from Brisbane to Coffs Harbour and then west of south from Coffs Harbour to Sydney where it joined the Front depicted in Fig. 1d. Surface temperature peaked near 26°C where the current was strongest and fell off by about 1°C on the seaward side of the southward flow. This behaviour is seen in Fig. 3c where the temperature falls towards the centre of the ridge near the 225km mark. Proceeding further, the surface temperature climbs back to a peak of 26°C at the position of the northward baroclinic current on the eastern side of the poleward meander near the 350km mark. The cooler surface water near 24°C residing within the cyclonic current ring, lies between the 375 and 675 km marks. Once again as the baroclinic current rises the surface temperature rises to peak near 26°C at the 750km mark. We have therefore traced hot northern water advected on the strong currents shown in Fig. 1c, south from Brisbane, around the poleward meander near Sydney, and then north and east around the cyclonic eddy centred on 157.5°E. This warm stream has a temperature from 1 to 4°C higher than adjacent surface water.

The final summer surface temperature data discussed in this paper are those for experiment 4, Fig. 4, which may be correlated with the dynamic height pattern of Fig. 1d. One notes immediately the extrusion of very warm (greater than 25°C) surface water along the 190 dyn cm isobar representing the Front near 34°S; this feature thins and splits near 155.5°E into a northward branch around the high in Fig. 1d and a south eastward branch along the Front. This hot water advected from the north is only one of the two sea surface temperature markers which show the position of the Front. The second identifying marker is horizontal temperature gradient which, on Fig. 4, lies just south of the band of 25-26°C water out to 156°E and then marks the south eastward stream. The distortion of isothermal surfaces in the thermocline has been shown to be most marked near the Tasman Front and there is an instance here where we are persuaded that deep-sea upwelling occurred. We believe this produced the crescent of very cool 21-22°C water near 34°S, 155°E on Fig. 4. The vertical isotherm section (not shown here) from the cruise track cutting the Tasman Front shows a wedge of cool water rising from about 120m depth north of the 190 dyn cm isobar to surface south of the Front.

Careful comparison of Figs. 4 and 1d shows other correlations mainly in the form of pooling of isothermal water near centres of pressure anomaly and stretching of surface isotherms along regions of strong geostrophic currents. Without the benefit of hindsight supplied by Fig. 1d these correlations, far from the Front, could not be automatically forecast with confidence. One can be reasonably confident however that sea surface temperature patterns near the East Australian Current and the Tasman Front can be interpreted usefully.

3.7. Some satellite observations.

In this section we present two satellite infra red photographs of areas in the Tasman sea which coincide with oceanographic data taken from surface vessels, thereby allowing comparisons to be made. We are seeking to show that the surface temperature effects observed from ships can also be observed remotely, from satellites.

Figure 5 is a NOAA-4, VHRR photograph taken on 13 October 1977. HMAS Diamantina was steaming in consort with HMNZS Tui from Brisbane to the site of an acoustic experiment east of Sydney near that time. Ships' thermograph and XBT data show that the warm plume in Fig. 5 along 153.5°E north of 32°S marks the East Australian coastal current with a surface temperature higher than the flanking water by 2 to 2.5°C, being advected by a geostrophic current increasing from 70cm s^{-1} at 30°S to 150cm s^{-1} at 32°S. Ships' XBT data also confirm that the current left the coast at 31.5°S to become a zonal stream crossing 154°E at 32°S. Figure 5 shows that out near 156.5°E the zonal stream bifurcates to form one segment heading north with a warm branch centred on 156.5°E and one segment heading south and then east to terminate at about 157.5°E. The northward branching may be linked to the topography as suggested by Godfrey and Robinson's (1971) numerical study; the edge of the Tasman abyssal plain has seamounts along 156°E between 30 and 34°S while in broader terms the edge of the Tasman abyssal plain lies roughly parallel to the Australian coast between 26 and 34°S. The bifurcation is quite like that shown in Fig. 1d and also the termination of the warm plume in the southward and eastward branch near 157.5°E on Fig. 5 is quite like the termination of the 25-26°C water near 156-157°E in Fig. 4. Notice that further east in Fig. 4 the Front is then marked by a straightforward surface temperature gradient. If similar behaviour applies in Fig. 5 then the Front is visible out to 161°E along the interface between South-Coral and Tasman Sea surface water. If we accept this then we can postulate that the cold water forms an equatorward (cyclonic) meander with a trough lying along the line 35°S, 160°E to 32°S, 160.5°E.

Figure 6 is a NOAA day infra red photograph for 14 November 1978 and the interpretation is far less straightforward than for Fig. 5. We rely on some CSIRO cruise results (RV Sprightly cruises SP15/78, 17-29 November 1978; SP 17/78, 9-11 December 1978) for a preliminary description although these data were taken only within 100km of the coast. The Sprightly data show that the East Australian Current flowed south between 27 and 29°S along the coast at speeds of about 1m s^{-1}; the current then left the coast at 29.5°S and diverted to the south east. This explains the origin of the thermal front on Fig. 6 entering the top of the picture at 154°E. This front converges with the coastline at 28.5°S, (off the photograph) as observed from RV Sprightly on 24-25 November 1978. We see on Fig. 6 that this branch of the current continues seaward across 155°E at 30.5°S and then the front meanders eastward between 30 and 31°S. South of this thermal front there is a very large pool of cool surface water centred near 31.5°S, 155°E. A filament of this surface water is advecting to the north east across 31°S, 157°E and beyond, where one can see billows as if the filament was contorted by a shear current. To the west of the pool of cool water, along the coast there is a thin stream of hot water parallel to the coast from 29.5°S to Sugarloaf Point (32.5°S) and continuing southward to 34°S where it blends with an intense eastward front. The data from SP 15/78 and SP 17/78 show there was a south east to eastward jet near 34°S, 152°E fed by (and lying between) a cyclonic disturbance to the south and an anticyclonic disturbance to the north. On Fig. 6 we see what we call the Tasman Front between 34 and 35°S out to 157°E where cloud cover obscures the picture. Finally, there is a cool equatorward intrusion of Tasman Sea water between the eastern edge of the photograph and about 158°E, extending north to 31°S.

Apparently the East Australian Current system was split into two eastward meandering components. One component left the coast near 28.5°S to meander east along 30-31°S while the Tasman Front lay between 34 and 35°S to then meander north around the cyclonic intrusion. It is reasonable to assume these two branches joined at the top of the intrusion to flow across 159°E near 30-31°S. It is interesting to compare Figs. 5 and 1b which show data taken four weeks apart. The main feature of the Tasman Front in mid November (Fig. 5) is still present in mid December (Fig. 1b): in Fig. 1b the Front leaves the coast near 34°S and then meanders north around a cyclonic intrusion, as it did in mid November.

In this section we have seen that a satellite study of the Tasman Front will be valuable and that there are two key features to be seen from space which can be easily associated with the Front: one is very warm northern water advected south along the path of the current while the other is the inherent difference in temperature between surface waters of South-Coral and Tasman Sea origin near the Front.

3.8. Scales of the motion and linearity.

The zonal wavelength of the meander patterns in Figs. 1 can be determined easily by eye and is about 370km, with not much variation between the four experiments. This is in good agreement with determinations made from structure function analyses (Andrews, 1979). We now consider propagation speeds and the linearity of an internal baroclinic wave model for these meanders.

Assume the baroclinic pressure anomaly is given by

$$y = y_0 \exp(i(kx+\ell y+wt)) \quad , \qquad (3)$$

where y_0 is the amplitude ; $k = 2\pi/370\text{km} = 1.7\text{X}10^{-5}\text{m}^{-1}$ and w is the angular frequency. If we use Lighthill's (1969) normal mode theory, and the observation that k is much larger than ℓ, the classical dispersion relation for the first internal mode is

$$w = -\beta k/(k^2+1/\mu^2) \quad , \qquad (4a)$$

where

$$\mu = (gH_1/f^2)^{1/2} \quad , \qquad (4b)$$

is the Rossby radius of deformation, H_1 is the eigendepth for the first mode, and f is the Coriolis parameter with a gradient of β. Andrews (1979) has computed the eigendepth off Sydney, H_1 =79cm, so the Rossby radius of deformation is μ = 33.4km at latitude 35°S. The ratio of the wavelength of the meanders of the Tasman Front to deformation scale meanders is therefore $1/k\mu = 1.8$. The phase speed,

$$c_p = w/k = -\beta/(k^2+1/\mu^2) \quad , \qquad (5a)$$

is 1.6cm s^{-1} westward while the group velocity,

$$c_g = \partial w/\partial k = c_p(1-(\mu k)^2)/(1+(\mu k)^2) \qquad (5b)$$

is 0.8 cm s^{-1} westward. These phase and group velocities of about 1.4 and 0.7 km day^{-1} are an order of magnitude smaller than the speeds at which fronts are generally observed to move, albeit sporadically; and the time scale $T = 370\text{km}/c_p$=9months is an order of magnitude too large: Hamon (1962,1968b) found a period more like 20 to 50 days applied while Hamon, Godfrey and Greig (1975) found fronts, or current patterns, move at around 9 km day^{-1}. Indeed, the front near J on Fig. 1c moved south at 15km day^{-1} during the four days between the aircraft survey and crossing by HMAS Kimbla while the front near H similarly moved west at about 20 km day^{-1}.

We cannot then look to linear theory to explain observed rates of change. Nonlinear processes transfer energy between wavenumbers by causing small eddies to cluster into ordered, deformation scale motion, or by destabilising large length scale planetary waves and zonal flows. Rhines (1973,1977) uses the wave steepness, ϵ, as a measure of the importance of these nonlinear processes. In the present case steepness is calculated from the ratio of the field accelerations to the local accelerations:

$$\epsilon = U_i \frac{\partial u_j}{\partial x_i} \Big/ \frac{\partial u_j}{\partial t} \qquad (6)$$

where U and u may belong to different spectral components and the i and j directions may be different. Repeated indices do not imply summation. For a zonal meandering current we should investigate u_j = northward geostrophic current and x_i = east distance, whereupon (6),(3) and (4) give

$$\epsilon = Uk/w = U(k^2+1/\mu^2)/\beta \qquad (7)$$

Here U is the r.m.s. depth-averaged velocity associated with the zonal flow.

We know that separated eddies in the East Australian Current system originate from a system with a wavelength of 1.8 times the deformation scale wavelength and we know that, on separating, they collapse to deformation scale eddies (Andrews and Scully-Power, 1976; Andrews, 1979). So we might, a priori, expect wave steepness of order unity or greater. The averaged pressure drop across the Front was earlier noted to be about 30cm; while the eddies and meanders disperse this across a band up to, at most, 600 or 700km wide. Hence a scale for U, from the geostrophic relation and the shapes of current profiles (Andrews, 1979) is about 2cm s^{-1}. On using this value in eq(7) we find ϵ is about 1.25 and we conclude that nonlinear processes are important in any dynamical interpretation of the Tasman Front.

To recapitulate, the ratio of the length scale of the meander pattern to the natural length scale (Rossby radius of deformation) is 1.8 so that it is only after the eddies detach from the Front that they assume the natural length scale. Secondly the steepness of the wave pattern is about 1.25 so the frontal dynamics are nonlinear ; in simple terms it seems that the effects of the meanders is to disperse the dynamic height change sufficiently broadly that the nonlinear influence is kept within reasonable bounds.

3.9. Discussion.

It seems clear that a zonal band about 600km wide centred near 33 or 34°S contains a meandering front stretching from Australia to New Zealand. Prior to our experiments, one could have expected this to be the case for a number of reasons. Firstly, time and space averaged maps of dynamic height in the south west Pacific show a broad zonal flow (e.g. Reid, 1961 but notably Wyrtki 1962,1974) which passes north of New Zealand. Secondly, spatial fluctuations appear in single cruise data from these latitudes when they have not been averaged; we have two complete temperature sections across the Tasman between Sydney and North Island (20-25 March 1976 and 3-7 April 1978; not presented here) which show essentially the same behaviour as Figs. 3a and 3b. Furthermore we have a temperature section (4-7 September 1978) from Bass Strait to the North Cape of North Island which does not show significant fluctuations. Thus there seemed to us to be a southern limit to the area where eddies are formed. The possibility of the existence of a northern limit as well and therefore of a zonal band, was established by the CSIRO in

1960 (Anon, 1962). They took a section at latitude 34°S from Sydney to New Zealand (3-8 February 1960) which showed typical eddy fluctuations and a similar section along 30°S from Australia to 170°E (18-22 March 1960) wherein there were no regular eddy fluctuations.

Now these historical data are fragmented and only presented a case for conducting the present investigation. However, if we couple the historical data with the data we present here and with Stanton's (1976) investigation, there is no doubt that the Tasman Front is a permanent feature joining the East Australian Current across the top of North Island (presumably) into the southern limb of the South Pacific subtropical gyre. Thus our faith in the integrity of the East Australian Current is restored; if an observer stands on the Australian coast near Coffs Harbour he will see a southward current at times near the coast (Fig. 1c) and at times further out to sea (Fig. 1a). It appears from present and historical data that the current will rarely cross the Tasman after leaving the coast further north. Whichever the case, it seems likely to us that a complex meandering system will always be found through which a western boundary current threads its way into the Tasman Front. It is the complexity of the meanders which led Hamon and Tranter(1971) to question the significance of the East Australian Current in the total circulation in the western South Pacific.

Warren's (1970) arguments are now very compelling. Essentially he took Welander's (1959) Sverdrup solution, which ignored the meridional barrier posed by New Zealand, and pondered the most likely real effect of New Zealand on that solution: Welander's interior solution across the portion of the South Pacific between New Zealand and South America would require a supply of water to the equatorward circulation from a western boundary current at the partial barrier (New Zealand). This in turn must be fed from the Tasman Sea west of New Zealand; but since there is no local wind stress curl there, the only flow can be zonal. This in turn implies the East Australian Current must leave the Australian coast at the latitude of the North Cape of North Island (34°S) where a zonal flow is required to supply the New Zealand western boundary current. We conclude that topography (New Zealand) and wind stress (the Sverdrup solution) play the dominant role in establishing the Tasman Front observed by us and others. This has been a brief presentation of Warren's argument which suffered from deficiencies in the wind stress data, and the spatial scale (5 degree squares) used by Welander (1959) and from excluding both the effects of stratification and bottom topography.

Cox (1975) was able to quantify Warren's (1970) arguments by using a 2 degree grid with Hellerman's (1967) improved annual mean wind stress field. Although he ran a full numerical model of the world ocean he paid particular attention to the circulation in the South Pacific and he used Warren's paper as a framework for discussing the circulation there. His first experiment with a homogeneous ocean reproduced neither the East Australian Current nor the Tasman Front. In his second experiment he used the observed averaged stratification and constrained it to be invariant with time. The result was the same; no Current and no Front developed west of New Zealand. He started his third experiment with the same averaged stratification but allowed it to change with time; i.e. he allowed baroclinic adjustment to evolve. In this case a broad East Australian Current developed transporting $22X10^6 m^3 s^{-1}$ south, all of which abruptly turned east as a zonal flow at the latitude of the North

Cape of North Island and continued as a western boundary current along east New Zealand. This set of three numerical experiments strongly suggests the following roles for wind stress, topography and stratification: the curl of the wind stress produces a basic Sverdrup circulation in the interior which is qualitatively and quantitatively adequate as a first approximation for the time averaged transport. New Zealand and Australia form the western meridional barrier along which must flow the western boundary current required to close the interior solution. A baroclinic adjustment (the Tasman Front) is required across the Tasman Sea to connect the two separated boundary currents; the baroclinic adjustment is responsible for differences like those on Figs. 2. Thus we may say that the difference in density structure (i.e. the Tasman Front) is maintained essentially because of the wind driven circulation in the central and eastern South Pacific Ocean and the nature of the split western boundary.

This is the circulation picture on time and space scales which exclude eddying mesoscale motion. In discussing these smaller scales we would have to consider the creation and intensification of meanders in a zonal baroclinic flow over topography. It is fairly clear now that wind stress is important only insofar as it sets up the interior circulation over the South Pacific Ocean, and does not play a primary role in the creation of meanders. We find that we cannot progress much further than simple scale arguments and these merely show that both baroclinic and topographic processes can be important. The exclusivity of poleward meanders near the Australian continental separation point simply results from the poleward flowing coastal current being forced to flow eastward near latitude 34°S, and this exclusivity is probably aided by the peculiar channel like topography described in section 7. We would also expect the currents to meander on crossing the Lord Howe Rise and the Norfolk Ridge. Even on a flat bottomed ocean, the wave steepness is sufficiently large that eddy formation, as simulated numerically by Rhines (1977) must occur. There is sufficient observational data now to investigate the relative effects of the bottom and baroclinic adjustment in this region of the western South Pacific by constructing a baroclinic -barotropic-topographic numerical model.

A potential tool for monitoring the currents and eddies exists with satellite photographs. The two thermal effects, advected hot northern water and a horizontal jump in temperature across the Front, are associated with a baroclinic front in the thermocline and swift geostrophic currents. It should be possible to obtain valuable satellite time series data on the positions of the thermocline fronts through the correlation between surface and deep structure; the major drawback is the extreme cloudiness of the area. We shall know more about the possibilities of infra red monitoring at the conclusion of the Heat Capacity Mapping Mission investigation.

We have given only approximate figures for current speeds and volume transports because we were interested principally in demonstrating that the continuous or time averaged flow from Australia into the subtropical South Pacific gyre is only about half the figure generally assumed. It is usual to take a compilation of volume transport calculations and treat them statistically to obtain a figure for the mean transport; typically then, (see Andrews, 1979) for the East Australian Current one arrives at a figure of between 20 and $40 \times 10^{6} m^{3} s^{-1}$ for a reference level of 1300 dbar from 35 individual transport calculations. Our data show that the larger transport calculations are associated with eddies near the Tasman Front which recirculate a lot of the water and a more realistic figure for the trans-Tasman transport is $15X10^6 m^3 s^{-1}$. This figure is small compared with transports in other western boundary currents and with what is expected for the western South Pacific. It seems quite possible therefore that there are other contributions to the subtropical gyral transport southward from flows along meridional barriers like the Lord Howe Rise and the Norfolk and Kermadec Ridges.

4. STATUS OF HCM-051 IMAGE PROCESSING

4.1 Photographic Image Processing

To date (30 April 1980) we have received over 400 IR images and about half that number of daylight visual images in photographic form. These photographic images are needed to assess the potential of the IR image. They are of limited scientific use in so far as direct comparison with ground truth data is concerned, because the photographic image has too low a temperature resolution to pick up anything but major (oceanographic) fronts. However, these images are essential to data assessment, choice of priority and co-ordinate correction. The process of photographic image processing at the user end is far from trivial and a flow chart is shown in Fig. 7 to the point where an order for a computer-compatible tape (CCT) is dispatched to NASA. The significant achievements of this process are

a. filing and listing the image information with assessed priority,
b. construction of a coordinate grid to cover the image, along with calculated corrections to NASA coordinates based on known landmarks and,
c. dispatch of CCT order to NASA.

4.2 Computer-compatible Tape (CCT) Processing

Upon receipt of a CCT the process shown in Fig. 8 is begun. Apart from bookkeeping, the first aim of this process is to map the tape and identify the various files. Following this, a "statistics" program is run on the IR image. This program obtains a mean temperature $\bar{t}$ and standard deviation s over 20 x 20 pixel squares over the complete image. That is, $\bar{t}$ and s are calculated for 6048 elements of the image. These maps of $\bar{t}$ and s are printed out in matrix form such that the print-out sheets can be put together to conform approximately to the shape of the original image. Thus the photographic image and the $\bar{t}$ matrix printout can be studied side by side and in a matter of seconds the desired range of apparent (HCM-IR) temperature for an enhanced image can be read off. Naturally, for 20 x 20 pixel elements that cover boundaries such as land/sea or cloud/surface, the values of $\bar{t}$ are meaningless. However, these values are characterised by a high value of s and in these cases a series of asterisks is substituted. We are presently using 2°C as the allowable limit for s.

It is quite possible, although not usually needed, to contour the $\bar{t}$ matrix. Portion of this printout is shown, contoured and colour-coded for temperature, in Fig. 9 for image 117-03470-2. We shall use this particular image to illustrate the rest of the enhancement process. Note that except for every tenth value, the tens of degrees figure is omitted from the $\bar{t}$ output. We can see from Fig. 9 that the useful temperature range (as recorded on the HCM-CCT) is 10.0 to 14.8°C. In this case we are only interested in the top right-hand quarter of the total image. Land and cloud are of no use to us. The whole, un-enhanced, image as supplied by NASA is reproduced as Fig. 11, together with the overlay coordinate grid computed by us (Fig. 10). Moreton and N. Stradbroke Is. (off Brisbane, Qld.) are clearly visible at about 27° 30'S, 153° 30' E with colder water (cold is white, hot black in these images) between the islands and the mainland.

The next step in CCT processing is to create an enhanced image tape in a format suitable to CSIRO's Division of Mineral Resources Photowrite image facility. This task has two main elements. Firstly, the required tape data has a totally different format to the original CCT. Secondly, we require enhanced data. The images we obtain from the photowrite are based on the 19 step exponential grey scale. Each step corresponds to an increase of exp(0.1732) in the corresponding digital level with level 19 (RANRL notation, which is the reverse of that of CSIRO) corresponding to black from a digital value of 255. All levels below 8 (value of 40) are virtually clear and indistinguishable (running under CSIRO program "Denis") leaving about 10 useful grey level steps. To date, the useful temperature range from each image has been confined to a range of less than 5°C. Thus we can let each grey level step correspond to a change of 0.5°C.

To transform the original CCT data to enhance (0.5° step values) we apply the following transformations:

CCT digital values → temp. values t (according to NASA formula)

Choose the mid-range temp., t_m, from the "Stats" $\bar{t}$ printout.

let $t' = t - t_m$

and $t_k = 2t' + 14$ (0.5° steps)

then $V_e = \text{Exp}\ (0.1732 \times (13.0 + t_k))$

where V_e is the digital value $0 \leq V_e \leq 255$ for CSIRO Photowrite. For example, for image ''7-03470-2, we chose the mid temperature $t_m = 13.0°C$ (actually we should have used 12.5°C). Level 19 (black) is then generated for all $t \geq 15.5°C$ and the image becomes essentially clear (level 8) for all $t \leq 10.0°C$. This enhanced image is reproduced as Fig. 12.

5. AN ENHANCED IR IMAGE 21 AUG 1978.

Fig. 12 shows a daytime IR image digitally enhanced by the process outlined in the previous section. It can be compared to the image prior to this enhancement shown in Fig. 11. The image shows a front marking the southern edge of a broad tongue of water warmer (on the surface) than 13.0°C (according to HCM data). This tongue extends south to about 29° 15'S and has an eastern boundary around 156°E. It would appear that HCM IR temperatures are under-reading by at least 5.5°C and the tongue really represents surface water warmer than 18.5°C. Fronts are maintained by current shear, so this demarkation is indicative of a current flowing south just offshore from Moreton Island, moving further offshore as we progress south and flowing eastward by latitude 29° 15'S. The current then turns and flows northward at about 155° 45'E. At latitude 27° 20'S the front (and current) swings eastward again. Considerable structure is evident inside the tongue. At the top of the image surface water warmer than 14.5°C (HCM) can be seen extending northward. A patch of cooler (< 12.5°C) water intrudes into the warm tongue between 26° and 27°S, 154° to 155°E. This patch ends in a narrow ribbon of cool water which is only visible in the enhanced image. It winds southward to 27°30'S, 154°E, almost joining the cool water east of the coast. It is too narrow to register on the $\bar{t}$ plot in Fig. 9 and cannot be readily seen in the un-enhanced image (Fig. 10). Just visible through the cloud southeast of 29°S, 156°E is a patch of water that is noticeably warmer than that further north or west around 154°E. This may be indicative of a separate eddy, but close examination of the image suggests that this patch of warm surface water may be connected to the northern tongue by a narrow neck around 29° 10'S, 155° 20'E. If so, we may conclude that the warm tongue expands out again under the cloud cover south of 29° 30'S in the vicinity of 156°E.

South of Cape Byron (28° 40'S) there appears to be little evidence of any East Australian Current running southward off the coast. The image clearly shows cooler water on the continental shelf adjacent to the coastline, but that is all. This interpretation of the IR image is confirmed by the oceanographic data about two weeks prior to 21 August by CSIRO; these data are discussed in the next section.

6. COMPARISON OF IR IMAGE AND GROUND TRUTH DATA

As yet we have no enhanced images available for direct comparison (coincident time and place) with ground truth data. However, we can come close to that with the image for 21 Aug 78 (Fig. 9 - Fig. 12) C.S.I.R.O. conducted an oceanographic survey over this area during the period 5-18 August 1978. Fig. 13 shows a contour map of surface dynamic height obtained from this quasi-synoptic survey. The contours are in dynamic metres (rel. 1300 dbar) and clearly show a tongue of warm (sub-surface) water extending from 26°S to 31°S between 154°E and 157°E. This is a dynamic "high" zone (maximum dynamic height anomaly 2.30 m), as compared to, say, the dynamic "low" of 1.80 m marked as L1. The current flow turns east at about 31°S, 154° 30'E, which is further south than our initial estimate of 29° 15'S from the IR image. However, we should note that the oceanographic section east along 31°S was taken during the period 6-9 August, nearly two weeks before the IR image. We know that these fronts can move south/north at least 30 km/day, so it is quite possible that this front retreated from 31°S to 29°S in that period.

The close-spaced dynamic height contours running south from $27^{\circ}S$ to $31^{\circ}S$ in the vicinity of $154-155^{\circ}E$ indicate a strong southward surface current. We can expect this current to draw warm surface water around the tongue from the Coral Sea. Indeed this was the case and the warmer water is shown as a stippled region in Fig. 13. This water was measured to be in the range 22.1 to $22.7^{\circ}C$, the maximum reading being in the centre of the northern edge of the stippled region (in the vicinity of the dynamic high of 2.30m). Temperatures outside this main current flow were some $2^{\circ}C$ cooler, typically 19.5 to $21.6^{\circ}C$. Now, we would not expect this water to cool more than $0.5^{\circ}C$/month in August, so the maximum surface temperature north-east of Brisbane ($\sim 26^{\circ}30'$, $154^{\circ}30'$) would be unlikely to have been cooler than $21.5^{\circ}C$ on 21 August 78, the time of the IR image. We conclude that in this case the IR data are under-reading by nearly $7^{\circ}C$.

While major fronts may move 200 km in a week or two, the body of warm water shown by the oceanographic survey cannot disappear in that time. Thus it is encouraging to see that, with respect to this comparison of IR image and survey data, the same major features are evident in both sets of data. The IR data has the advantage of being synoptic and continuous. There are many minor features in the enhanced image that no program of surveying by ship could hope to uncover.

7. THE NEED FOR SYNOPTIC (IR) DATA

The mesoscale features of the ocean such as these warm tongues, the EAC and the associated eddies can be considered as the "weather" of the ocean. These features are analogous in many ways to atmospheric weather patterns. Consider the time and distance scales: an atmospheric weather pattern may typically have a diameter of 2000 km and may move 500-1000 km/day. The time scale for these features is thus 2-4 days. The equivalent oceanographic features have wavelengths ~ 250 km and will move, say, 20 km/day. The time scale per pattern is thus ~ 12 days. We can say that one week in the ocean is approximately equivalent to one day in the atmosphere. Now, in order to predict the weather the various meteorological bureaux around the world have many thousands of observers making truly synoptic observations several times each day. In order to similarly predict the movement of ocean currents and eddies, we should observe them several times each week. Now consider that the sparse survey shown in Fig. 13 took 13 days to complete.

Contouring such data is often difficult because the mesoscale patterns shift while the observations are being made! While the time scale is, say, seven times easier for oceanographic work, the density of observations needed is $\sim$ 100 times that required for meteorological work. Thus the task of providing oceanographic forecasts on any kind of regular basis is obviously beyond classical oceanographic capabilities. Satellite observations solve both the spatial density and synoptic problems and also should solve the time sampling problem. It only remains to relate the IR observations adequately with the oceanographic structures and some giant steps can be taken toward regular oceanographic forecasting.

8. PRIORITIES OF HCM DATA PROCESSING AND JUSTIFICATION OF DATA NEEDS

Our first task is to maintain "good housekeeping" with respect to the flow of HCM-051 data. This means that images for any time/location can be readily identified, retrieved and the status of processing ascertained. This we have achieved and a status list for most of our data is given in the Appendix.

Our next priority is to compare HCM images with ground truth data so that we determine what we can and cannot see with the HCM images relative to our previous oceanographic analyses and to learn how to use HCM data to infer subsurface oceanographic structure. This problem will not be solved immediately, but we expect that HCM data will take us a good way along that path. It is apparent that to make these comparisons, we need CCT data in order to obtain enhanced images. We have noted many standard order images in which mesoscale structure appears to be absent because the sea surface temperature has not suited the standard grey scale. The CCT data required for this task have been listed as priority AA in the Appendix.

We already have some theories about the behaviour of the East Australian Current (EAC) and the Tasman Front. In particular, one of us (C.S.N.) believes that the flow of the EAC down the east coast of Australia may well be able to be predicted up to one year ahead by periodic monitoring of the Tasman Front. Initially we need to study the position of the Tasman Front on a regular (time-series) basis in order to see how the wave-like patterns moves with time. We believe that this front is an example of a baroclinic Rossby wave and as such, it should show a westward phase velocity. The only practicable way of confirming this movement (and indeed the regular existence of the front) is by a time series of satellite IR data. The HCM-051 data offer a unique opportunity to achieve this. For this we need a good time-series of observations extending over a year and we have selected the HCM data for this task as priority A.

There are many good images sufficiently clear of cloud that cover areas outside that of the Tasman Front or EAC and its associated eddies. Typically these are south of 38°S and some of them clearly show mesocale features associated with the Sub-tropical Convergence. This is an area of considerable interest, but is outside the immediate aims of HCM-051. We have classified these as priority B for CCT data. There is no doubt that important scientific work could be achieved using these data, both on the formation of eddies along this front and in determining the short-term and seasonal variations in the latitude of the convergence.

9. PUBLICATIONS

Section 3 has been submitted to the Journal of Physical Oceanography for publichation under the title, "Observations of the Tasman Front" by J.C. Andrews, M.W. Lawrence and C.S. Nilsson.

10. ACKNOWLEDGEMENTS

This work is a contribution to the Australian Defence Science and Technology Organisation's project DST 78/071 and DST 80/006 and the National Aeronautics and Space Administration's project HCM-051: Heat Capacity Mapping Mission. Data were collected at sea from HMAS Diamantina and HMAS Kimbla and from the air by Orion aircraft of 11 Squadron, 92 Wing based at RAAF Edinburgh. The AXBT surveys were supported by the U.S. Office of Naval Research and we wish particularly to thank Dr. R.E. Stevenson for his support. Mr. R. Schenk is thanked for his grid computing analyses. Dr. D.G. Nichol produced the digitally enhanced NOAA-4 infra red photograph. CSIRO Division of Mineral Resources produced the enhanced HCM photograph and have been particularly helpful.

11. APPENDIX: STATUS OF CCT PROCESSING (02 APR 80)

This section contains the output lists from the sorted image data on computer file.

PRIORITY AA

These images are needed for IMMEDIATE COMPARISON with existing GROUND-TRUTH data.

Image status data are divided into three groups for this priority, these groups are for CCT data which (1) have not yet been ordered, but soon will be, (2) have been ordered but not yet received and (3) have been received.

Status data can be interpreted as follows: G = grid made, O = CCT ordered, R = CCT received; absence of appropriate letters indicate the negative.

GROUP (1). C/C TAPES HAVE NOT YET BEEN ORDERED. BUT SOON WILL BE.

R	FR	DATE	LAT	LONG	DAY HHMM T	FL	AZ	P	STATUS	POS	ERR
09	415	160778	-2937	15547	081-15080-3			AA			
11	130	210778	-3001	15716	086-15010-3			AA			
11	028	220778	-3035	15236	087-15190-3			AA			
09	004	250778	-3154	15450	090-03470-2	31	317	AA			
10	037	260778	-3651	15131	091-04040-2	27	320	AA			
10	035	260778	-3044	14955	091-04050-2	32	316	AA			
10	040	260778	-2644	15942	091-14530-3			AA			
10	041	260778	-3250	15812	091-14540-3			AA			
10	039	270778	-3057	15408	092-15120-3			AA			
10	040	270778	-3702	15232	092-15130-3			AA			
10	313	310778	-3822	15332	096-03560-2	26	320	AA			
10	311	310778	-3215	15154	096-03580-2	32	316	AA			
10	309	310778	-2607	15025	096-03590-2	38	311	AA			
10	152	310778	-2723	16114	096-14460-3			AA			
10	153	310778	-3330	15943	096-14470-3			AA			
10	073	020878	-3646	14946	098-15240-3			AA			
10	063	270878	-3805	15231	123-03560-2	34	312	AA			
10	061	270878	-3200	15053	123-03580-2	39	307	AA			
10	068	270878	-2714	16014	123-14460-3			AA			
10	069	270878	-3322	15844	123-14470-3			AA			
10	013	280878	-3109	15442	124-15050-3			AA			
10	014	280878	-3716	15305	124-15070-3			AA			
10	046	080978	-3047	15256	135-15110-3			AA			
10	047	080978	-3654	15120	135-15130-3			AA			
10	068	060279	-2856	16022	286-02560-2	64	281	AA			
05	145	080279	-3244	15209	288-03320-2	62	285	AA	G		
05	159	100279	-4046	14549	290-04050-2	55	292	AA	G	28	-21
05	008	100279	-3118	15142	290-14570-3			AA	G		
05	009	100279	-3723	15005	290-14580-3			AA	G	38	-35
05	029	120279	-3429	15913	292-03060-2	60	288	AA	G	43	-25
05	027	120279	-2823	15741	292-03080-2	64	282	AA	G	259	-48
10	204	130279	-3155	15400	293-03250-2	61	286	AA			
10	202	130279	-2548	15231	293-03270-2	65	280	AA			
05	230	180279	-2853	15449	298-03190-2	62	285	AA	G	48	-35
10	024	190279	-3817	15243	299-03340-2	55	293	AA			
10	022	190279	-3211	15105	299-03360-2	60	288	AA			
10	095	210279	-3039	15000	301-15010-3			AA			
10	054	230279	-3301	15728	303-03110-2	58	290	AA			
10	052	230279	-2653	15558	303-03120-2	63	285	AA			
10	045	240279	-3858	15434	304-03270-2	53	295	AA			
11	242	240279	-3544	15340	304-03280-2	56	293	AA			
10	043	240279	-3252	15255	304-03290-2	58	290	AA			
10	041	240279	-2645	15124	304-03300-2	63	285	AA			
11	240	240279	-2938	15205	304-03300-2	61	287	AA			
10	057	250279	-3818	14952	305-03450-2	53	295	AA			

PRIORITY AA GROUP(1) CONTINUED

R	FR	DATE	LAT	LONG	DAY HHMM T	FL	AZ	P	STATUS	POS	ERR
10	063	250279	-3020	15616	305-14350-3			AA			
10	064	250279	-3626	15441	305-14370-3			AA			
05	139	010379	-2917	15346	309-03220-2	59	289	AA	G		

NUMBER OF IMAGES PRIORITY AA, GROUP(1) = 48

GROUP (2), C/C TAPES HAVE BEEN ORDERED BUT NOT RECEIVED AS OF 02 APR 80

B	FR	DATE	LAT	LONG	DAY HHMM T	FL	AZ	P	STATUS	POS	ERR
02	434	240778	-3016	15858	089-03290-2	32	316	AA	GO		

NUMBER OF IMAGES PRIORITY AA, GROUP(2) = 1

GROUP (3), C/C TAPES HAVE BEEN RECEIVED FOR THE FOLLOWING IMAGES

R	FR	DATE	LAT	LONG	DAY HHMM T	EL	AZ	P	STATUS	POS	ERR
11	131	210778	-3606	15541	086-15020-3			AA	P		
02	041	010878	-3001	15602	097-15040-3			AA	GOR	53	4
02	042	010878	-3606	15428	097-15060-3			AA	GOR	34	-12
04	015	290878	-3112	15005	125-15230-3			AA	GOR	45	-4
04	016	290878	-3719	14829	125-15250-3			AA	GOR	34	-6

NUMBER OF IMAGES PRIORITY AA, GROUP(3) = 5

NUMBER OF IMAGES PRIORITY AA= 54

PRIORITY A

These images are needed for IMMEDIATE AIMS of HCM-051.

Image status data are divided into three groups for this priority, these groups are for CCT data which (1) have not yet been ordered, but soon will be, (2) have been ordered but not yet received and (3) have been received.

Status data can be interpreted as follows: G = grid made, O = CCT ordered, R = CCT received; absence of appropriate letters indicates the negative.

GROUP (1). C/C TAPES HAVE NOT YET BEEN ORDERED, BUT SOON WILL BE.

R	FP	DATE	LAT	LONG	DAY HHMM T	FL	AZ	P	STATUS	POS	ERR
09	494	230578	-3854	15231	027-04100-2	22	0	A			
09	492	230578	-3249	15052	027-04120-2	27	316	A			
10	255	240578	-3052	15430	028-15190-3			A			
10	256	240578	-3700	15254	028-15210-3			A			
09	615	090678	-3102	15407	044-15190-3			A			
09	616	090678	-3708	15231	044-15200-3			A			
09	638	180678	-3147	15310	053-03590-2	27	319	A			
09	090	220678	-3307	15931	057-03340-2	26	320	A			
05	051	060778	-3612	15102	071-15230-3			A	G	32	-6
09	416	160778	-3542	15413	081-15090-3			A			
10	056	190778	-3057	15732	084-03360-2	31	317	A			
11	132	210778	-4210	15355	086-15040-3			A			
09	047	230778	-3636	14632	088-15380-3			A			
09	002	250778	-2546	15321	090-03490-2	37	312	A			
11	221	050878	-3540	16042	101-14410-3			A			
10	003	090878	-2600	15810	105-03270-2	40	309	A			
10	018	100878	-3241	15516	106-03430-2	34	313	A			
10	049	110878	-2632	16009	107-14490-3			A			
10	050	110878	-3239	15840	107-14510-3			A			
10	051	110878	-3845	15701	107-14520-3			A			
11	038	130878	-3111	14956	109-15260-3			A			
11	230	150878	-3748	15817	111-03340-2	31	315	A			
11	228	150878	-3141	15640	111-03360-2	36	311	A			
11	226	150878	-2532	15511	111-03380-2	42	307	A			
10	048	160878	-3837	15359	112-03520-2	30	316	A			
10	046	160878	-3231	15220	112-03540-2	36	311	A			
10	044	160878	-2622	15051	112-03560-2	41	307	A			
09	014	160878	-2715	16137	112-14420-3			A			
09	015	160878	-3322	16006	112-14440-3			A			
09	035	170878	-3025	15618	113-15010-3			A			
11	004	180878	-4242	14822	114-15220-3			A			
10	061	200878	-3008	15757	116-03290-2	39	308	A			
11	136	220878	-3123	15744	118-14540-3			A			
10	228	240878	-3756	14656	120-15310-3			A			
10	015	060978	-3917	15536	133-03440-2	35	309	A			
11	053	170978	-2736	16105	144-14390-3			A			
11	054	170978	-3344	15934	144-14410-3			A			
11	055	170978	-3950	15752	144-14420-3			A			
05	036	240978	-3037	15239	151-15100-3			A	G	53	11
11	020	290978	-3030	15407	156-15030-3			A			
11	021	290978	-3637	15231	156-15050-3			A			
11	022	290978	-4242	15043	156-15070-3			A			
11	026	300978	-3723	14744	157-15230-3			A			
05	212	031078	-3312	15201	160-03490-2	48	294	A	G	36	5
05	210	031078	-2707	15030	160-03510-2	52	289	A	G	104	4

PRIORITY A GROUP(1) CONTINUED

R	FR	DATE	LAT	LONG	DAY HHMM T	EL	AZ	P	STATUS	POS	FPR
05	155	051078	-2710	15154	162-15140-3			A	G	114	11
05	156	051078	-3317	15023	162-15150-3			A	G	52	8
11	107	301078	-3257	15839	187-14390-3			A			
05	344	081278	-2858	15137	226-15050-3			A	G	52	4
11	058	191278	-2622	15040	237-15090-3			A			
11	059	191278	-3229	14910	237-15110-3			A			
11	060	191278	-3836	14731	237-15120-3			A			
10	124	010179	-3559	15604	250-03230-2	62	279	A			
10	122	010179	-2953	15430	250-03250-2	64	274	A			
11	026	020179	-4407	15357	251-03390-2	57	286	A			
11	024	020179	-3802	15206	251-03410-2	61	281	A			
11	022	020179	-3157	15029	251-03430-2	63	276	A			
10	289	020179	-2638	15953	251-14300-3			A			
10	290	020179	-3247	15823	251-14320-3			A			
10	016	030179	-3211	15402	252-14500-3			A			
10	040	060179	-3900	15834	255-03150-2	60	282	A			
10	038	060179	-3255	15654	255-03170-2	63	277	A			
10	036	060179	-2649	15523	255-03190-2	65	272	A			
10	029	070179	-3014	16042	256-14240-3			A			
10	137	110179	-3241	15902	260-03100-2	63	278	A			
10	135	110179	-2635	15732	260-03110-2	65	272	A			
10	033	130179	-2701	15914	262-14330-3			A			
10	034	130179	-3308	15742	262-14350-3			A			
09	057	160179	-3156	16036	265-03020-2	64	278	A			
09	055	160179	-2550	15907	265-03040-2	66	273	A			
10	043	180179	-3810	15316	267-03360-2	60	284	A			
10	048	180179	-2714	16056	267-14260-3			A			
10	116	190179	-3027	15537	268-14440-3			A			
10	444	210179	-2943	16142	270-02560-2	65	277	A			
10	084	280179	-3251	15404	277-03260-2	63	282	A			
05	132	020279	-3252	15523	282-03200-2	63	283	A	G	109	-9
05	130	020279	-2646	15355	282-03210-2	66	278	A	G	134	-24
09	092	030279	-3858	15229	283-03360-2	58	289	A			
09	090	030279	-3253	15050	283-03380-2	62	284	A			
10	090	040279	-3011	15432	284-14450-3			A			
10	218	140279	-3849	15118	294-03410-2	56	292	A			
10	076	260279	-4350	14705	306-04020-2	48	300	A			
05	140	010379	-3524	15519	309-03200-2	55	294	A	G		
05	318	230379	-3530	15136	331-03300-2	48	303	A	G	31	11
11	132	270379	-3208	15647	335-03060-2	49	301	A			
11	130	270379	-2602	15519	335-03080-2	55	296	A			
11	014	090579	-3034	15346	378-03120-2	38	315	A			

NUMBER OF IMAGES PRIORITY A, GROUP(1) = 87

GROUP (2), C/C TAPES HAVE BEEN ORDERED BUT NOT RECEIVED AS OF 02 APR 80

R	FR	DATE	LAT	LONG	DAY HHMM T	EL	AZ	P	STATUS	POS	FPR
03	016	110678	-2531	15921	046-03310-2	32	314	A	GO		
03	036	140678	-3131	15526	049-15120-3			A	GO	58	3
08	006	170678	-3317	15806	052-03400-2	25	320	A	GO		
08	242	200678	-3004	15241	055-15240-3			A	GO	52	6
08	243	200678	-3611	15107	055-15250-3			A	GO	32	-7
08	244	200678	-4216	14920	055-15270-3			A	GO	12	-7
03	153	240678	-3359	15743	059-15000-3			A	GO		
02	436	240778	-3623	16033	089-03280-2	27	320	A	GO		

PRIORITY A GROUP(2) CONTINUED

R	FR	DATE	LAT	LONG	DAY HHMM T	EL	AZ	P	STATUS	POS	ERR
04	121	220878	-3054	15752	118-14530-3			A	GO		
04	244	260978	-3234	15928	153-03200-2	46	296	A	GO		
04	242	260978	-2628	15758	153-03220-2	51	292	A	GO		
08	[illegible]42	280978	-3400	15043	155-03560-2	46	297	A	GO	35	4
08	030	261078	-3122	15248	183-15040-3			A	GO	109	9
08	031	261078	-3728	15111	183-15060-3			A	GO	40	-1
08	127	301078	-2614	16017	187-14370-3			A	GO		
03	301	121278	-2607	15819	230-14400-3			A	GO		

NUMBER OF IMAGES PRIORITY A, GROUP(2) = 16

GROUP (3), C/C TAPES HAVE BEEN RECEIVED FOR THE FOLLOWING IMAGES

R	FR	DATE	LAT	LONG	DAY HHMM T	EL	AZ	P	STATUS	POS	ERR
08	105	270678	-3313	16102	062-03270-2	26	320	A	GOR		
08	103	270678	-2706	15932	062-03290-2	31	316	A	GOR		
03	089	280678	-3320	15631	063-03450-2	26	320	A	GOR		
03	087	280678	-2714	15501	063-03470-2	31	316	A	GOR	114	-14
03	079	300678	-3028	15533	065-15100-3			A	GOR	56	4
08	027	020778	-2649	16100	067-03220-2	32	316	A	GOR		
02	207	040778	-3946	15514	069-03550-2	20	323	A	GOR		
02	205	040778	-3341	15334	069-03560-2	26	320	A	GOR		
02	203	040778	-2734	15204	069-03580-2	32	316	A	GOR		
02	003	100778	-3940	15609	075-14590-3			A	GOR		
02	168	160778	-3007	15540	081-15080-3			A	GOR	14	6
02	169	160778	-3611	15405	081-15090-3			A	GOR	35	-9
02	004	180778	-2852	16134	083-03190-2	33	316	A	GOR		
02	012	220778	-2940	15250	087-15190-3			A	GOR	53	10
02	043	010878	-4211	15241	097-15080-3			A	GOR	13	-12
04	133	210878	-3016	15326	117-03470-2	39	308	A	GOR	103	-1
04	176	230878	-3021	15328	119-15110-3			A	GOR	55	4
04	177	230878	-3628	15153	119-15130-3			A	GOR	33	-6
04	056	160978	-3546	15725	143-03320-2	41	303	A	GOR		
04	054	160978	-2940	15552	143-03340-2	46	298	A	GOR	58	-9
04	034	170978	-3314	15941	144-14100-3			A	GOR		
04	033	170978	-2707	16112	144-14390-3			A	GOR		
04	144	230978	-2716	15802	150-14510-3			A	GOR		
04	145	230978	-3323	15631	150-14520-3			A	GOR		
04	238	250978	-3655	14625	152-15300-3			A	GOR	20	-5
08	192	290978	-3008	15413	156-15030-3			A	GOR	57	9
08	193	290978	-3615	15237	156-15050-3			A	GOR	35	1
08	151	300978	-3720	14744	157-15230-3			A	GOR	31	2
08	023	191078	-3332	15217	176-03460-2	51	288	A	GOR	29	3
08	021	191078	-2726	15045	176-03480-2	55	284	A	GOR	57	-5
08	033	201078	-3001	15558	177-14530-3			A	GOR	51	6
08	034	201078	-3607	15423	177-14550-3			A	GOR	44	2
08	015	251078	-3047	15728	182-14460-3			A	GOR		
08	016	251078	-3653	15552	182-14480-3			A	GOR		
08	128	301078	-3220	15847	187-14390-3			A	GOR		
		141178	0	0	202-03280-2			A	R		
01	138	141178	-2704	15422	202-03300-2	59	275	A	GOR	118	-14
06	120	151178	-2625	16027	203-14350-3			A	GOR		
06	121	151178	-3231	15857	203-14360-3			A	GOR		
06	122	151178	-3837	15719	203-14380-3			A	GOR		
06	092	171178	-3038	15013	205-15120-3			A	GOR	59	8
01	084	181178	-4317	16441	206-03010-3			A	GOR		

PRIORITY A GROUP(3) CONTINUED

R	FR	DATE	LAT	LONG	DAY HHMM T	EL	AZ	POS	FPR
06	135	191178	-3235	15701	207-03220-2	57	279		
06	133	191178	-2628	15531	207-03240-2	59	27		
06	116	241178	-3153	15812	212-03170-2	58	27		
06	114	241178	-2545	15643	212-03180-2	60	2		
06	007	291178	-3646	16052	217-03090-2	57			
06	005	291178	-3039	15915	217-03110-2	60			
07	114	051278	-3301	15644	223-03220-2	6		1	1
07	152	061278	-2713	16109	224-14280-3				
07	153	061278	-3320	15938	224-14300-3				
07	510	131278	-4423	14746	231-04070-2	6			
07	011	191278	-2552	15047	237-15090-3			100	1

NUMBER OF IMAGES PRIORITY A, GROUP(3) =

NUMBER OF IMAGES PRIORITY A= 156

PRIORITY b

These images are needed for LONG-TERM AIMS of HCM-051.

Image status data are divided into three groups for this priority, these groups are for CCT data which (1) have not yet been ordered, but soon will be, (2) have been ordered but not yet received and (3) have been received.

Status data can be interpreted as follows: G = grid made, O = CCT ordered, R = CCT received; absence of appropriate letters indicates the negative.

GROUP (1). C/C TAPES HAVE NOT YET BEEN ORDERED, BUT SOON WILL BE.

R	FR	DATE	LAT	LONG	DAY HHMM T	EL	AZ	P	STATUS	POS	ERR
09	490	230578	-2642	14923	027-04140-2	33	312	B			
10	126	250578	-4720	14602	029-04450-2	14	322	B			
10	124	250578	-4116	14402	029-04460-2	19	320	B			
10	151	100678	-4058	14357	045-04450-2	18	323	B			
09	088	220678	-2700	15802	057-03350-2	31	316	B			
10	208	010778	-4023	14447	066-04370-2	19	324	B			
09	482	050778	-3722	15001	070-04130-2	23	322	B			
05	052	060778	-4216	14916	071-15250-3			B	G	26	0
09	465	120778	-3131	14913	077-15330-3			B			
09	467	120778	-4339	14546	077-15360-3			B			
09	077	160778	-3604	14811	081-04180-2	25	321	B			
09	417	160778	-4146	15227	081-15110-3			B			
09	429	170778	-4550	14638	082-04330-2	16	325	B			
09	431	170778	-3125	15048	082-15260-3			B			
09	433	170778	-4333	14722	082-15290-3			B			
10	058	190778	-3704	15909	084-03350-2	25	321	B			
09	037	220778	-4203	14659	087-04270-2	21	323	B			
09	048	230778	-4240	14444	088-15400-3			B			
09	008	250778	-4407	15819	090-03440-2	19	323	B			
09	006	250778	-3801	15628	090-03450-2	25	320	B			
10	039	260778	-4257	15319	091-04020-2	21	323	B			
10	042	260778	-3855	15632	091-14560-3			B			
10	027	270778	-4230	14838	092-04200-2	21	322	B			
10	041	270778	-4306	15044	092-15150-3			B			
10	604	280778	-2529	15055	093-15280-3			B			
10	606	280778	-3740	14750	093-15320-3			B			
10	607	280778	-4344	14600	093-15330-3			B			
10	154	310778	-3935	15803	096-14490-3			B			
10	068	020878	-4050	14511	098-04310-2	24	320	B			
10	074	020878	-4250	14759	098-15260-3			B			
10	022	100878	-4453	15849	106-03400-2	23	321	B			
10	020	100878	-3848	15655	106-03410-2	28	317	B			
10	016	100878	-2633	15346	106-03450-2	40	309	B			
11	039	130878	-3717	14819	109-15280-3			B			
11	040	130878	-4323	14630	109-15300-3			B			
11	232	150878	-4353	16008	111-03330-2	25	319	B			
09	031	170878	-4211	15032	113-04090-2	27	317	B			
09	036	170878	-3631	15443	113-15020-3			B			
09	037	170878	-4237	15255	113-15040-3			B			
11	003	180878	-3637	15010	114-15200-3			B			
10	226	240878	-2542	15002	120-15280-3			B			
10	015	280878	-4321	15116	124-15080-3			B			
11	010	020978	-4235	15038	129-04070-2	31	312	B			
11	008	020978	-3630	14850	129-04090-2	37	308	B			
10	017	060978	-4521	15730	133-03420-2	30	312	B			

PRIORITY B GROUP(1) CONTINUED

B	FR	DATE	LAT	LONG	DAY HHMM T	EL	AZ	P	STATUS	POS	ERR
10	029	060978	-4632	15735	133-14390-3			B			
10	048	080978	-4300	14932	135-15140-3			B			
10	003	090978	-3858	14609	136-15310-3			B			
11	056	170978	-4555	15556	144-14440-3			B			
11	008	190978	-4058	14513	146-04250-2	38	305	B			
10	119	240978	-4147	14654	151-04180-2	38	303	B			
05	037	240978	-3644	15103	151-15110-3			B	G	34	5
05	038	240978	-4249	14915	151-15130-3			B	G	20	0
11	011	280978	-4334	15330	155-03530-2	38	303	B			
11	009	280978	-3731	15140	155-03550-2	43	299	B			
11	025	300978	-3117	14921	157-15220-3			B			
05	216	031078	-4519	15536	160-03460-2	38	302	B	G		
05	214	031078	-3916	15341	160-03480-2	43	298	B	G		
05	157	051078	-3922	14843	162-15170-3			B	G	43	9
11	442	151078	-4300	14851	172-04090-2	43	296	B			
10	266	211078	-4029	14509	178-04210-2	47	293	B			
11	106	301078	-2650	16008	187-14380-3			B			
11	108	301078	-3902	15658	187-14410-3			B			
11	101	311078	-2632	15543	188-14550-3			B			
11	103	311078	-3843	15234	188-14590-3			B			
11	104	311078	-4447	15042	188-15000-3			B			
11	018	161178	-4159	14910	204-04020-2	52	287	B			
11	016	161178	-3553	14723	204-04040-2	55	282	B			
05	083	271178	-4017	14644	215-04090-2	55	283	B	G	15	16
10	171	081278	-4046	14509	226-04140-2	57	283	B			
05	345	081278	-3504	15003	226-15070-3			B	G	22	-4
05	346	081278	-4110	14819	226-15080-3			B	G	13	-5
10	126	010179	-4203	15750	250-03220-2	58	284	B			
10	291	020179	-3853	15643	251-14340-3			B			
10	292	020179	-4459	15449	251-14350-3			B			
10	012	030179	-4200	14844	252-03580-2	58	285	B			
10	010	030179	-3555	14659	252-03590-2	62	280	B			
10	015	030179	-2603	15532	252-14400-3			B			
10	017	030179	-3818	15222	252-14510-3			B			
10	018	030179	-4423	15029	252-14530-3			B			
10	098	040179	-4104	14356	253-04160-2	59	284	B			
10	031	070179	-4226	15720	256-14270-3			B			
10	126	100179	-4231	14204	259-04260-2	58	286	B			
10	131	100179	-3829	14528	259-15200-3			B			
10	139	110179	-3846	16041	260-03080-2	60	283	B			
10	066	130179	-3746	15124	262-03440-2	61	282	B			
11	430	140179	-4005	14733	263-04010-2	59	285	B			
10	068	150179	-4717	14523	264-04170-2	54	291	B			
10	066	150179	-4114	14325	264-04190-2	58	286	B			
09	051	150179	-3735	14727	264-15120-3			B			
09	052	150179	-4340	14537	264-15140-3			B			
10	045	180179	-4413	15506	267-03350-2	56	289	B			
10	049	180179	-3321	15924	267-14270-3			B			
10	050	180179	-3928	15742	267-14290-3			B			
09	019	200179	-3826	14855	269-15050-3			B			
09	020	200179	-4431	14702	269-15070-3			B			
11	234	230179	-4519	15623	272-03280-2	55	291	B			
11	232	230179	-3916	15429	272-03300-2	59	286	B			
11	230	230179	-3311	15249	272-03310-2	63	281	B			
11	228	230179	-2705	15120	272-03330-2	66	275	B			
05	126	250179	-3932	14523	274-04060-2	59	287	B	G	11	16

PRIORITY B GROUP(1) CONTINUED

B	FR	DATE	LAT	LONG	DAY HHMM T	EL	AZ	P	STATUS	POS	ERR
10	088	280179	-4500	15735	277-03220-2	55	292	B			
10	086	280179	-3856	15543	277-03240-2	59	287	B			
11	145	300179	-3632	15132	279-14530-3			B			
11	146	300179	-4237	14946	279-14540-3			B			
05	136	020279	-4501	15855	282-03160-2	54	293	B	G		
05	134	020279	-3857	15702	282-03180-2	58	288	B	G		
09	094	030279	-4502	15421	283-03340-2	54	294	B			
09	088	030279	-2647	14919	283-03390-2	66	278	B			
10	143	040279	-4306	14908	284-03530-2	55	292	B			
10	091	040279	-3617	15258	284-14470-3			B			
10	092	040279	-4222	15112	284-14480-3			B			
10	057	050279	-4126	14402	285-04120-2	56	291	B			
10	062	050279	-3637	14818	285-15050-3			B			
10	063	050279	-4241	14631	285-15070-3			B			
05	232	180279	-3500	15621	298-03170-2	58	290	B	G		
10	026	190279	-4422	15435	299-03330-2	50	298	B			
10	056	230279	-3907	15908	303-03090-2	53	295	B			
11	244	240279	-4150	15526	304-03260-2	51	298	B			
10	074	260279	-3746	14514	306-04030-2	54	295	B			
05	105	300379	-4017	14524	338-03580-2	41	309	B	G	18	1
11	012	280479	-2708	15458	367-03060-2	44	309	B			
05	152	290479	-4131	15411	368-03200-2	30	320	B	G		
05	162	300479	-4012	14910	369-03390-2	31	320	B	G	15	12
10	284	040579	-4429	15622	373-03140-2	25	323	B			
10	278	040579	-2616	15126	373-03190-2	43	310	B			
09	163	050579	-4228	15109	374-03330-2	27	323	B			

NUMBER OF IMAGES PRIORITY B, GROUP(1) = 127

GROUP (2), C/C TAPES HAVE BEEN ORDERED BUT NOT RECEIVED AS OF 02 APR 8

B	FR	DATE	LAT	LONG	DAY HHMM T	EL	AZ	P	STATUS	POS	ERR
03	123	100678	-3711	14755	045-15380-3			B	GO	26	-11
03	018	110678	-3138	16048	046-03290-2	27	318	B	GO		
03	309	120678	-3307	15637	047-03470-2	25	319	B	GO		
03	307	120678	-2701	15508	047-03480-2	31	315	B	GO	125	-17
03	069	150678	-3238	15032	050-15310-3			B	GO	47	0
08	008	170678	-3922	15945	052-03390-3			B	GO		
03	267	200678	-4014	14619	055-04330-2	19	323	B	GO		
04	134	210878	-3623	15502	117-03450-1	33	313	B	0		
04	117	210878	-4025	15947	117-14380-3			B	GO		
04	118	210878	-4630	15749	117-14400-3			B	GO		
04	246	260978	-3839	16108	153-03180-2	42	301	B	GO		
08	046	280978	-4607	15422	155-03520-2	36	305	B	GO		
08	044	280978	-4004	15225	155-03540-2	41	301	B	GO	22	-9
08	194	290978	-4220	15050	156-15060-3			B	GO	18	-6
08	139	311078	-4247	15121	188-15000-3			B	GO	24	-1

NUMBER OF IMAGES PRIORITY B, GROUP(2) = 15

GROUP (3), C/C TAPES HAVE BEEN RECEIVED FOR THE FOLLOWING IMAGES

B	FR	DATE	LAT	LONG	DAY HHMM T	EL	AZ	P	STATUS	POS	ERR
08	021	150578	-3617	14546	019-15520-3			B	GOR	20	-20
08	113	230678	-4650	15820	058-14450-3			B	GOR	0	0
03	147	250678	-2959	15410	060-15170-3			B	GOR	53	7

PRIORITY B GROUP(3) CONTINUED

R	FR	DATE	LAT	LONG	DAY	HHMM	T	EL	AZ	P	STATUS	POS	ERR
02	209	040778	-4550	15710	069	03530	2	14	326	B	GOR		
02	004	100778	-4543	15413	075	15010	3			B	GOR		
02	027	210778	-2957	15717	086	15010	3			B	GOR		
04	158	180878	-3626	15013	114	15200	3			B	GOR	34	-8
04	159	180878	-4231	14826	114	15220	3			B	GOR	19	-6
04	137	210878	-4228	15649	117	03440	2	28	316	B	GOR		
04	135	210878	-3623	15502	117	03450	2	33	313	B	GOR		
04	123	220878	-4306	15426	118	14570	3			B	GOR		
04	178	230878	-4234	15005	119	15150	3			B	GOR	23	-3
04	017	290878	-4325	14639	125	15270	3			B	GOR	15	-6
04	235	070978	-4517	15253	134	04000	2	30	312	B	GOR		
04	241	070978	-4258	15407	134	14560	3			B	GOR		
04	012	120978	-4143	15552	139	14490	3			B	GOR		
04	035	170978	-3921	15801	144	14420	3			B	GOR		
04	146	230978	-3930	15450	150	14540	3			B	GOR		
04	147	230978	-4535	15254	150	14560	3			B	GOR		
04	233	250978	-4243	14238	152	04360	2	38	304	B	GOR		
08	190	051078	-4613	14648	162	04220	2	38	302	B	GOR		
08	188	051078	-4010	14451	162	04240	2	43	298	B	OR		
08	042	161078	-4150	14356	173	04270	2	44	295	B	GOR	19	19
08	041	271078	-4206	14249	184	04310	2	47	292	B	GOR		
08	129	301078	-3825	15709	187	14410	3			B	GOR		
06	142	141178	-3917	15733	202	03270	2	53	285	B	GOR		
06	137	191178	-3842	15841	207	03210	2	54	283	B	GOR		
06	518	271178	-4019	14645	215	04090	2	55	283	B	GOR	19	14
07	039	111278	-4520	15419	219	03430	2	33	287	B	GOR		
06	037	011278	-3915	15224	219	03450	2	56	282	B	GOR		
07	012	191278	-3200	14917	237	15110	3			B	GOR	43	4
07	013	191278	-3807	14739	237	15120	3			B	GOR	30	-1

NUMBER OF IMAGES PRIORITY B, GROUP(3) = 32

NUMBER OF IMAGES PRIORITY B= 174

TOTAL NUMBER OF IMAGES LISTED= 384

References.

Andrews, J.C., 1976: The bathythermograph as a tool in gathering synoptic thermohaline data. Aust.J.Mar. Freshwat.Res., 27,405-415.

Andrews, J.C.,1979: Eddy structure and the West and East Australian Currents. Flinders Institute for Atmospheric and Marine Sciences, Research Rept. 30, 172pp.

Andrews, J.C., and P.D. Scully-Power, 1976: The structure of an East Australian Current anticyclonic eddy. J. Phys.Oceanogr.,6, 756-765.

Anonymous, 1962: Oceanographical Investigations in the Pacific Ocean in 1960. CSIRO Division of Fisheries and Oceanography, Oceanographical Cruise Rept. No. 5.

Cox, M.D., 1975: A baroclinic numerical model of the world ocean: preliminary results. In: Numerical models of Ocean Circulation, National Academy of Sciences, Washington, D.C., 107-120.

Denham, R.N., and Crook, F.J.,1976: The Tasman Front. N.Z.J. Mar. Freshwat.Res., 10,15-30.

Godfrey, J.S., and A.R. Robinson, 1971: The East Australian Current as a free inertial jet. J.Mar.Res., 29,256-280.

Hamon, B.V., 1962: The spectrums of mean sea level at Sydney, Coffs Harbour and Lord Howe Island. J. Geophys.Res., 67,5147-5155.

Hamon, B.V., 1968a: Temperature structure in the upper 250 metres in the East Australian Current area. Aust.J. Mar.Freshwat.Res., 19, 91-99.

Hamon, B.V., 1968b: Spectrum of sea level at Lord Howe Island in relation to circulation. J.Geophys.Res., 73,6925-6927.

Hamon, B.V., J.S. Godfrey and M.A. Greig, 1975: Relation between mean sea level, current and wind stress on the east coast of Australia. Aust.J.Mar. Freshwat.Res., 26, 389-403.

Hellerman, S., 1967: An updated estimate of the wind stress on the world ocean. Mon.Weather Rev., 95,607-626 (corrected in 1968, 96, 63-74).

Lighthill, M.J., 1969: Dynamic response of the Indian Ocean to onset of the southwest monsoon, Phil.Trans.R. Soc.Lond., 265, (1159), 45-92.

Nilsson, C.S., J.C. Andrews and P.D. Scully-Power, 1977: Observations of eddy formation off east Australia. J.Phys.Oceanogr., 7, 659-669.

Nilsson, C.S., and G.R. Creswell, 1979: Formation and evolution of east Australian eddies. Submitted to Progress in Oceanography.

Reid, J.L.Jr., 1961: On the geostrophic flow at the surface of the Pacific Ocean with respect to the 1000 decibar surface. Tellus, 13, 489-502.

Rhines, P.B., 1973: Observations of the energy-containing eddies and theoretical models of waves and turbulence. Boundary Layer Met., 4, 345-360.

Rhines, P.B., 1977: The dynamics of unsteady currents. In: The Sea, Vol.4, Ideas and observations on progress in the study of the seas, E.D. Goldberg, Editor. John Wiley and Sons, pp. 189-318.

Stanton, B.R., 1975: Vertical structure in the mid-Tasman Convergence Zone. N.Z.J.Mar.Freshwat.Res., 9, 63-74.

Stanton, B.R., 1976: An oceanic frontal jet near the Norfolk Ridge northwest of New Zealand. Deep-Sea Res., 23, 821-829.

Warren, B.A.,1970: General circulation of the South Pacific. In: Scientific exploration of the South Pacific, Warren S. Wooster, Editor. National Academy of Sciences, Washington, D.C., pp 33-49.

Wyrtki, K., 1962: Geopotential topographies and associated circulation in the western South Pacific Ocean. Aust.J.Mar.Freshwat.Res., 13, 89-105.

Wyrtki, K., 1974: The dynamic topography of the Pacific Ocean and its fluctuations. Hawaii Institute of Geophysics, Report HIG-74-5, 19pp.

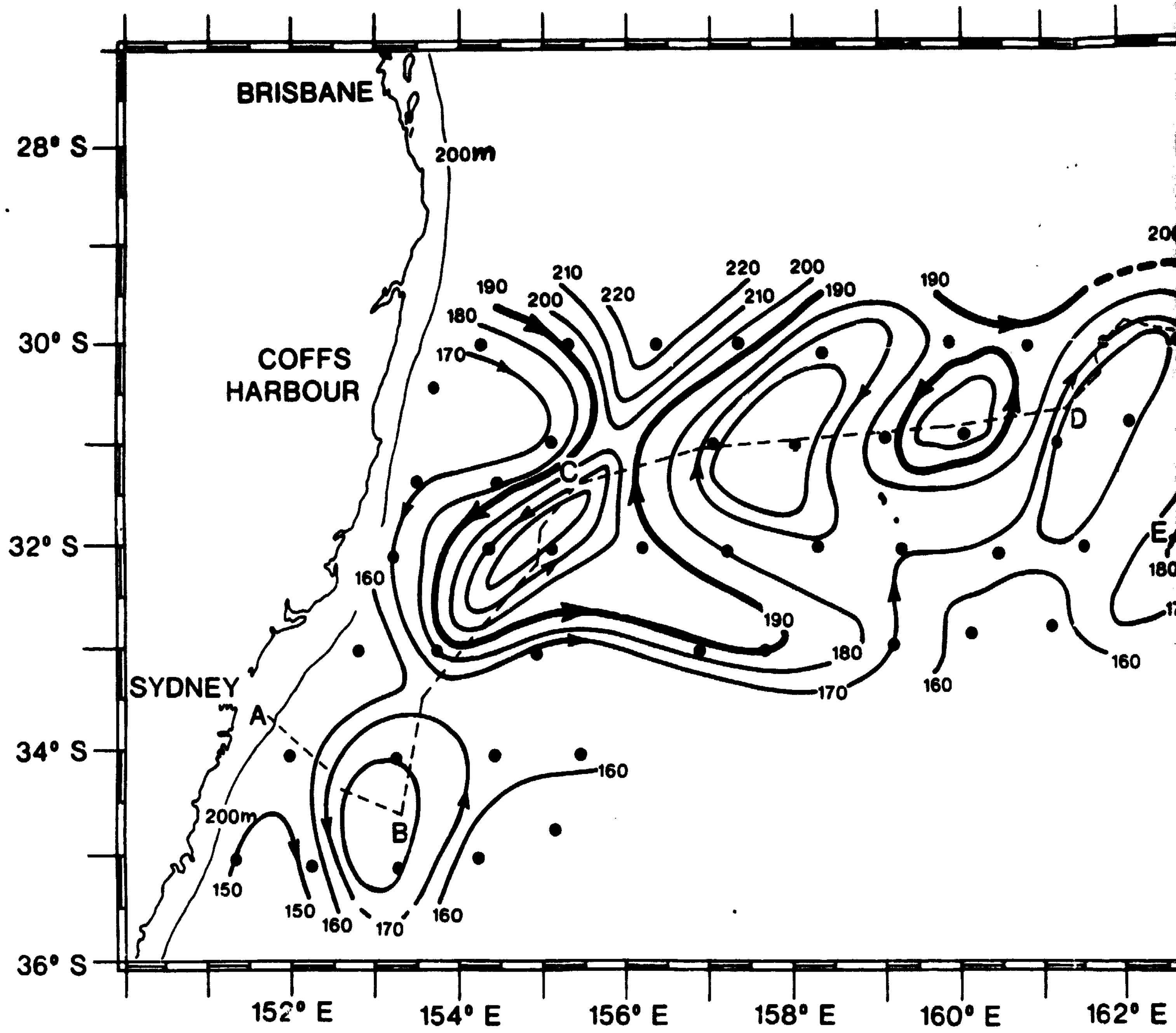

Figure 1a: Dynamic height anomaly (0 re 1300 dbar in dyn cm) ded
probes along ABCDEF (HMAS Diamantina, 4-11 Sept 78), a
rectangle shows the location of the Tasman Front foun

FOLDOUT FRAME

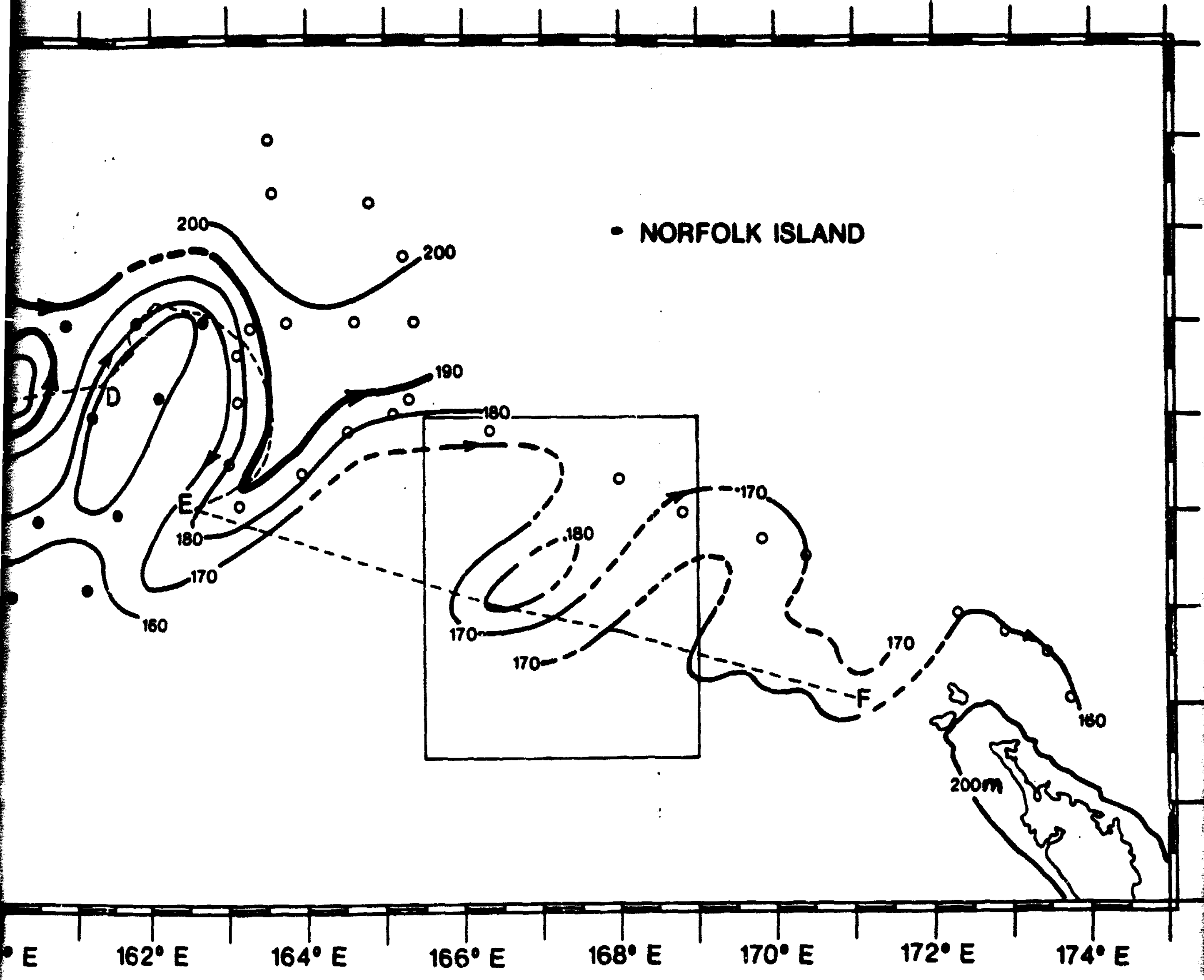

bar in dyn cm) deduced from AXBT probes (29 Aug 78, filled circles), XBT
., 4-11 Sept 78), at open circles (HMAS Diamantina, 13-18 Sept 78). The
Tasman Front found by Stanton (1976).

FOLDOUT FRAME 2

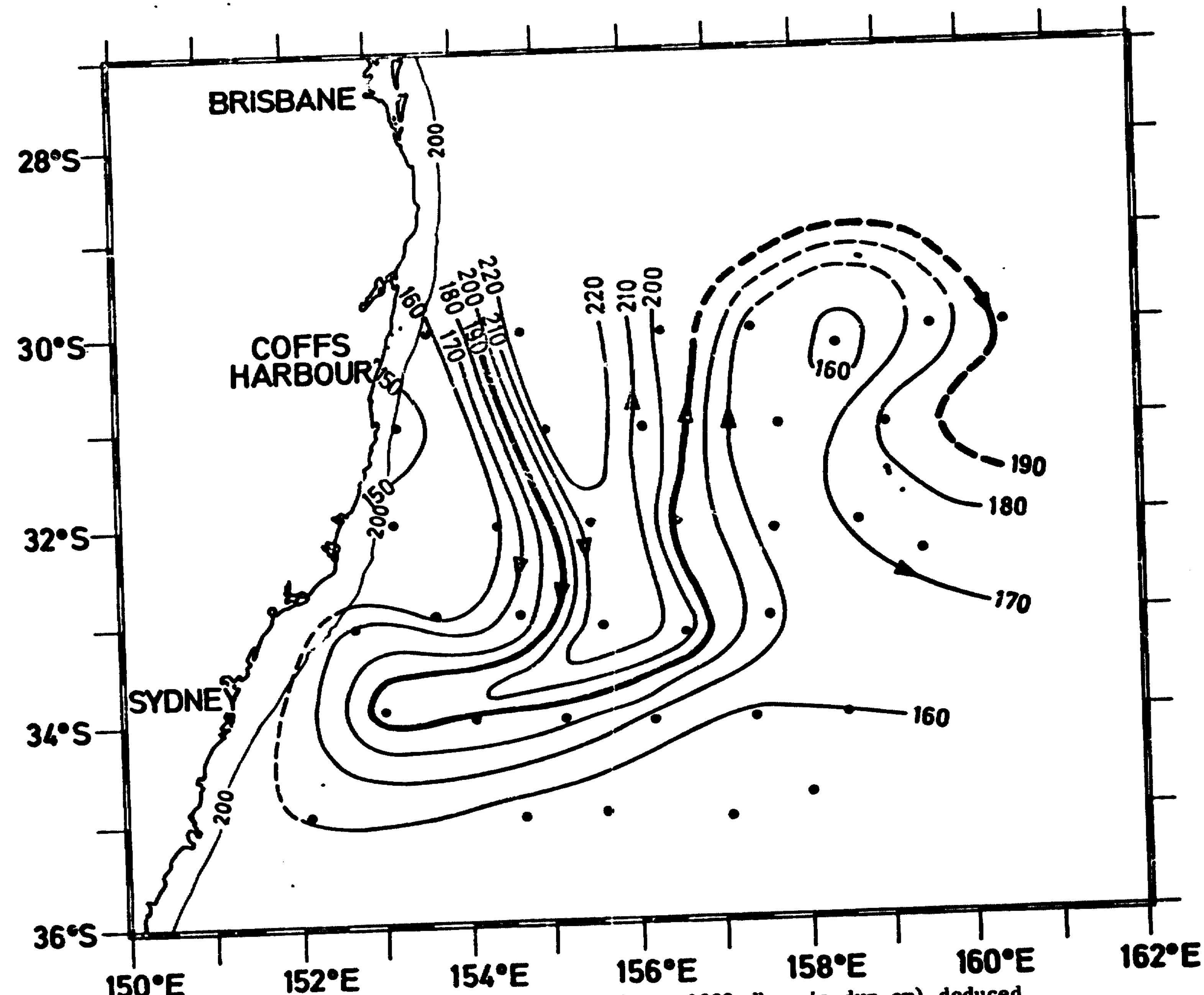

Figure 1b: Dynamic height anomaly (0 re 1300 dbar in dyn cm) deduced from AXBT probes (13 Dec 78, filled circles).

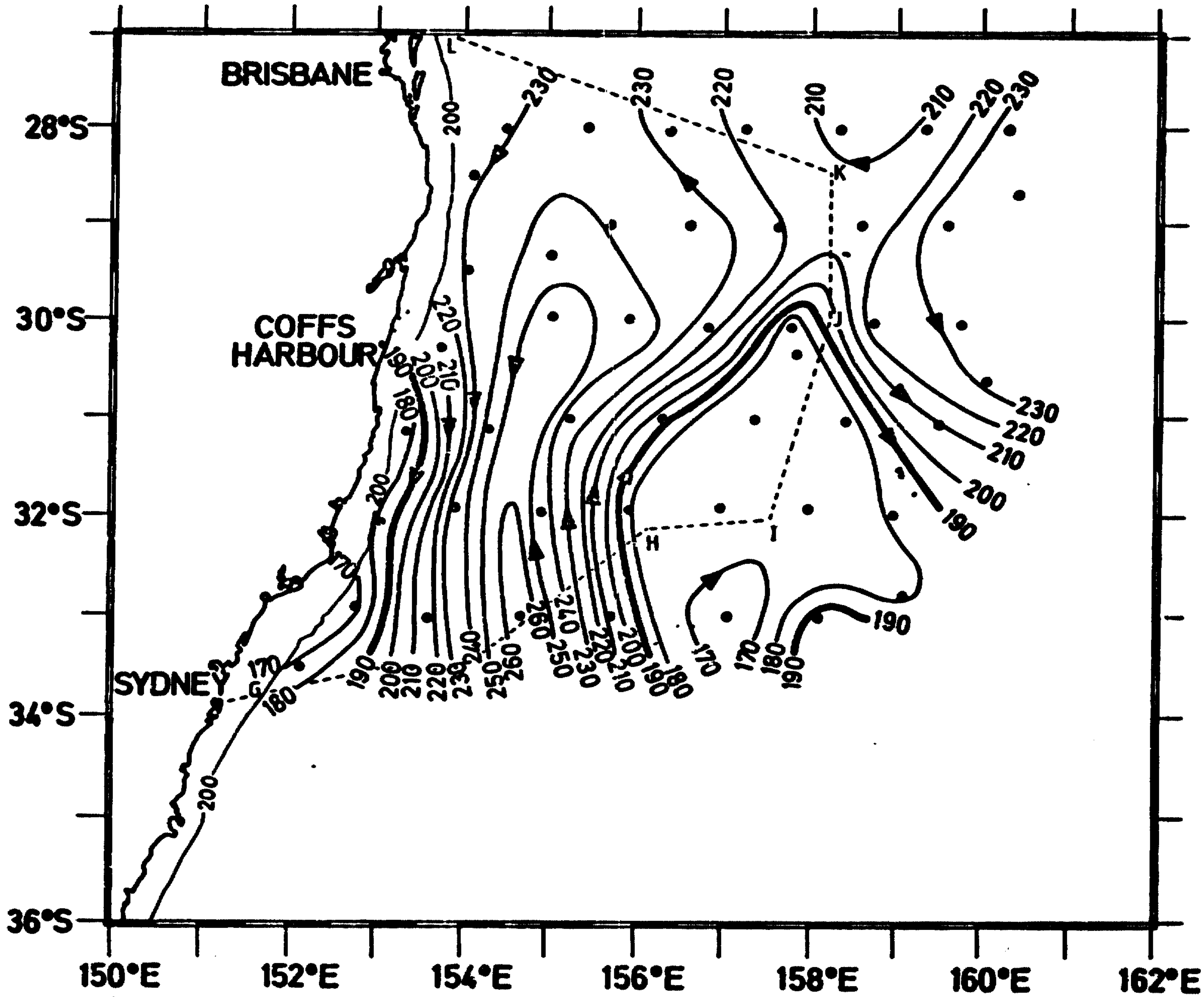

Figure 1c: Dynamic height anomaly (0 re 1300 dbar in dyn cm) deduced from AXBT probes (8 Feb 79, filled circles) and XBT probes along GHIJKL (HMAS Kimbla, 11-19 Feb 79).

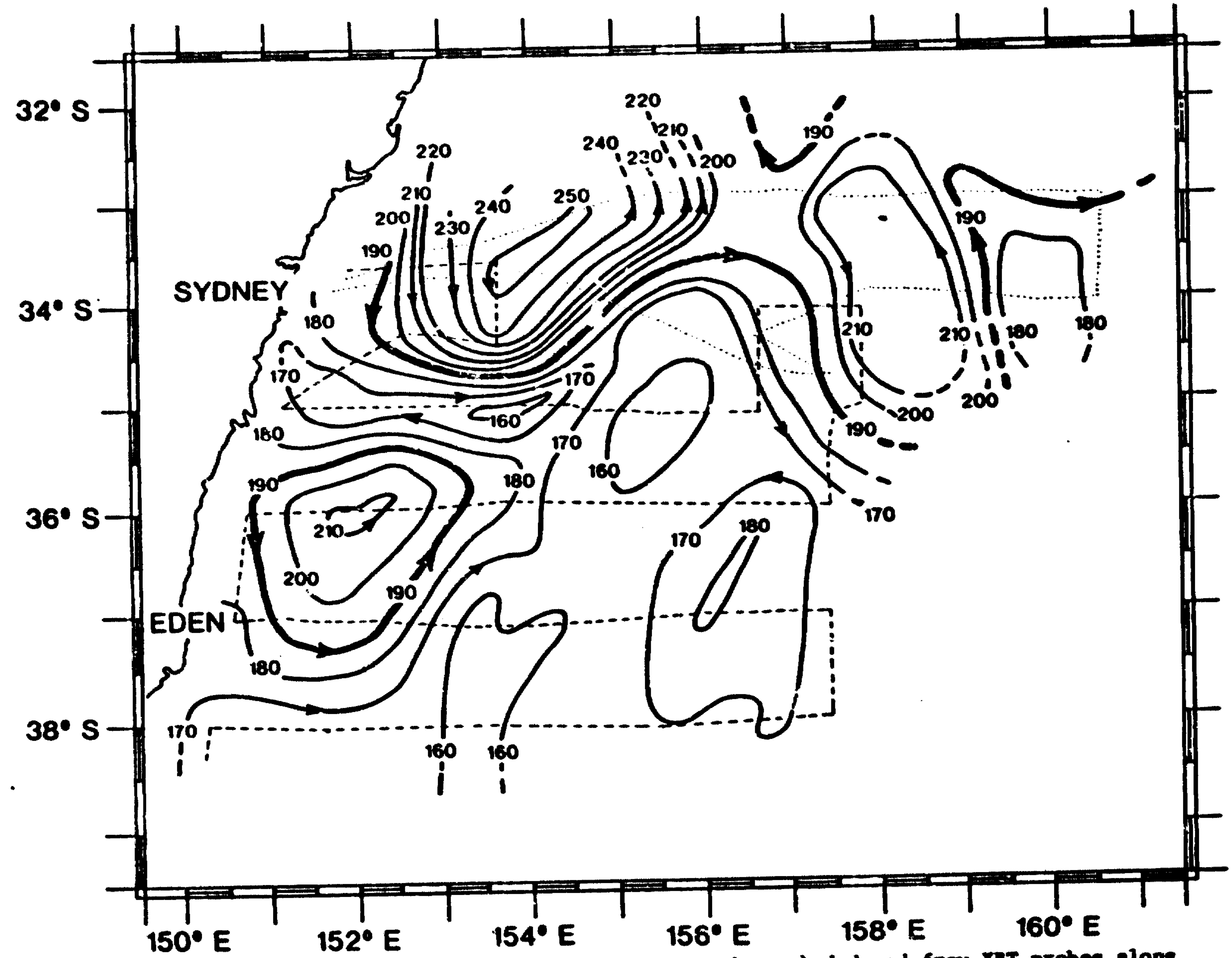

Figure 1d: Dynamic height anomaly (0 re 1300 dbar in dyn cm) deduced from XBT probes along the track of HMAS Diamantina (dashed 22 Feb-1 Mar 79; dotted 8-12 Mar 79).

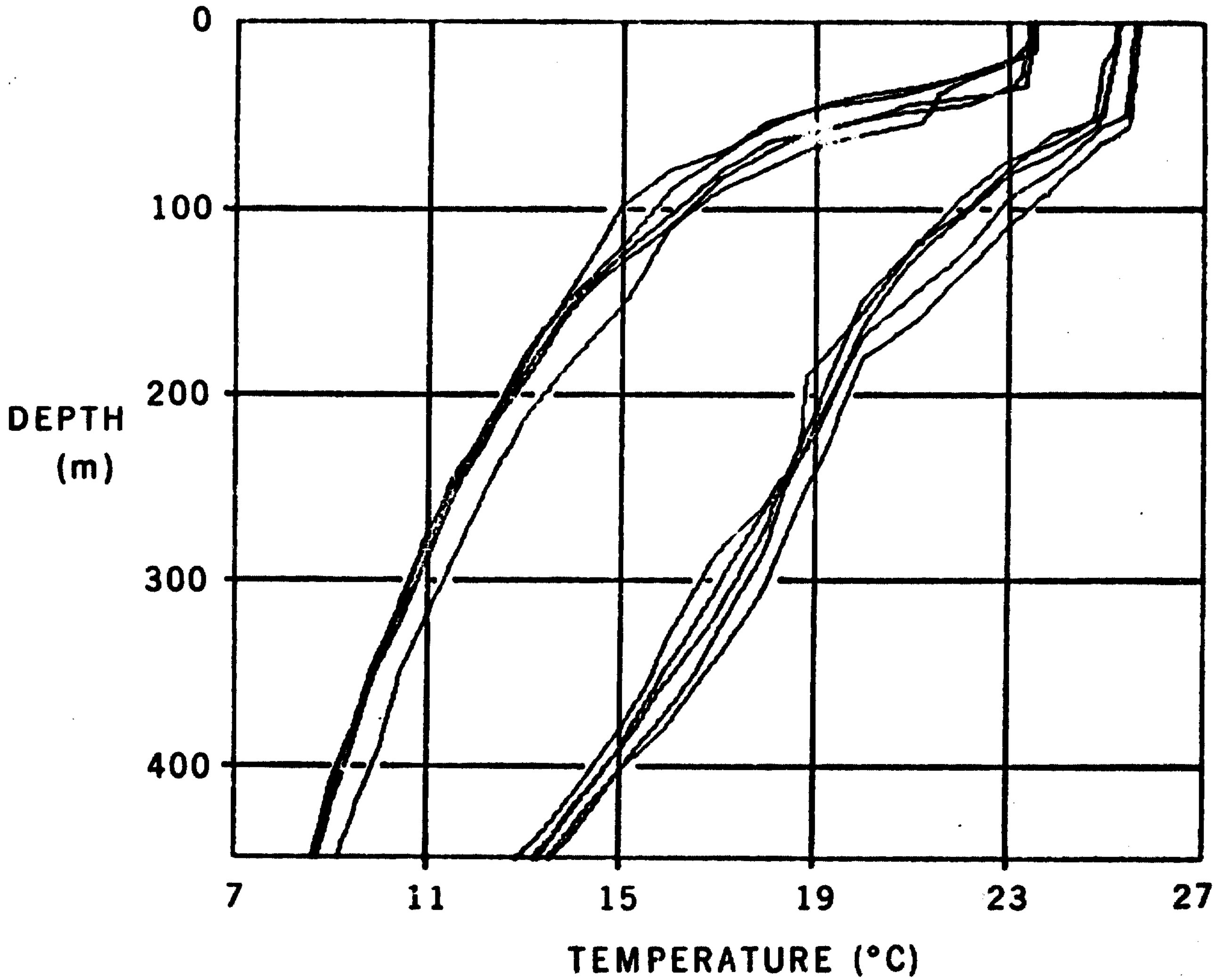

Figure 2a: XBT profiles from quiescent regions north and south of the Tasman Front. The warm profiles are from leg KL of Fig. 1c between 155.4 and 156.3^{o}E; the cold profiles are from the leg along 36^{o}S in Fig. 1d between 155 and 156.2^{o}E.

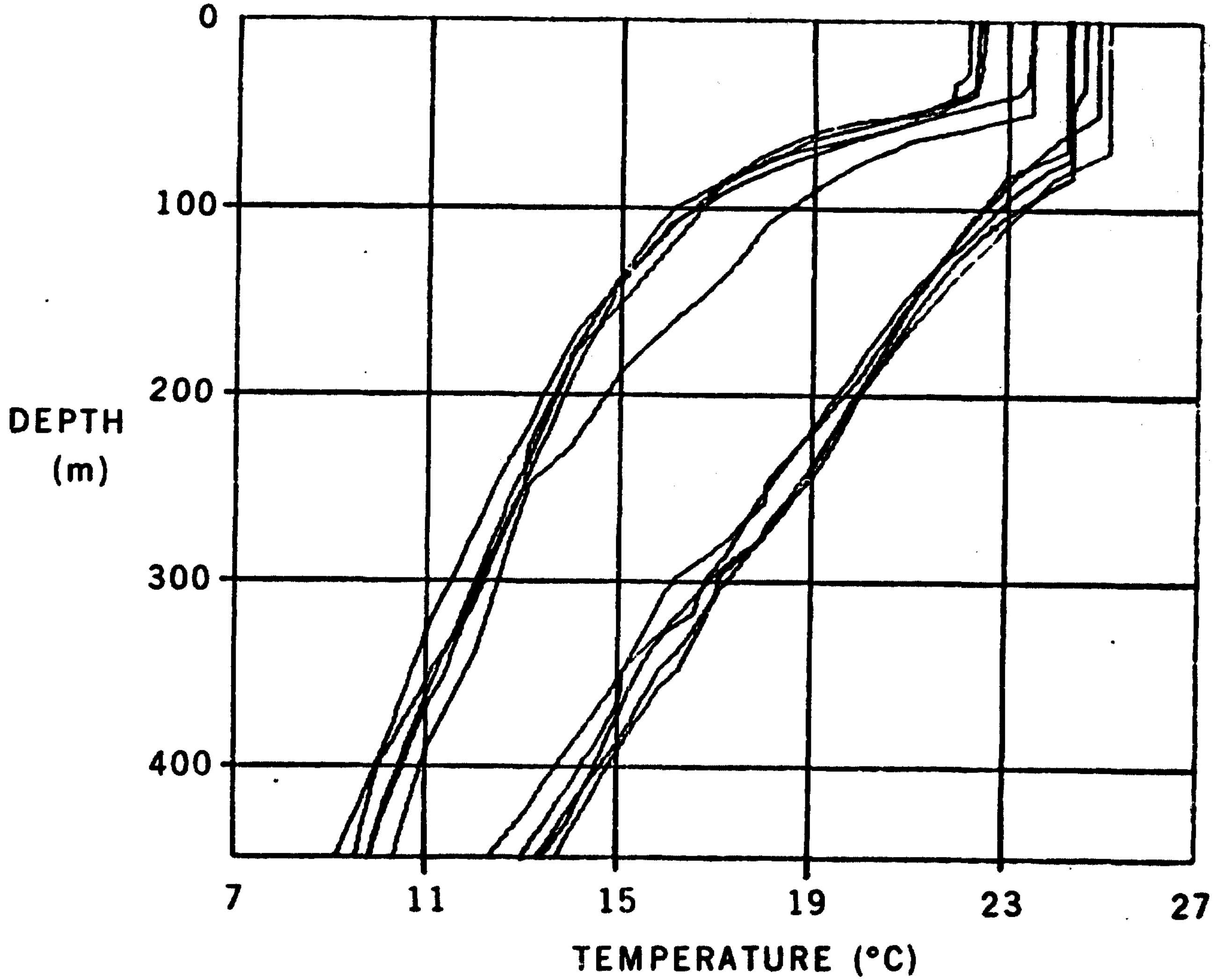

Figure 2b: XBT profiles from the centres of a warm eddy on the warm side and a cold eddy on the cold side of the Tasman Front. The profiles are from the leg along 34°S in Fig. 1d; the warm profiles lie between 157.7 and 158.7°E while the cool profiles lie between 159.6 and 160.5°E.

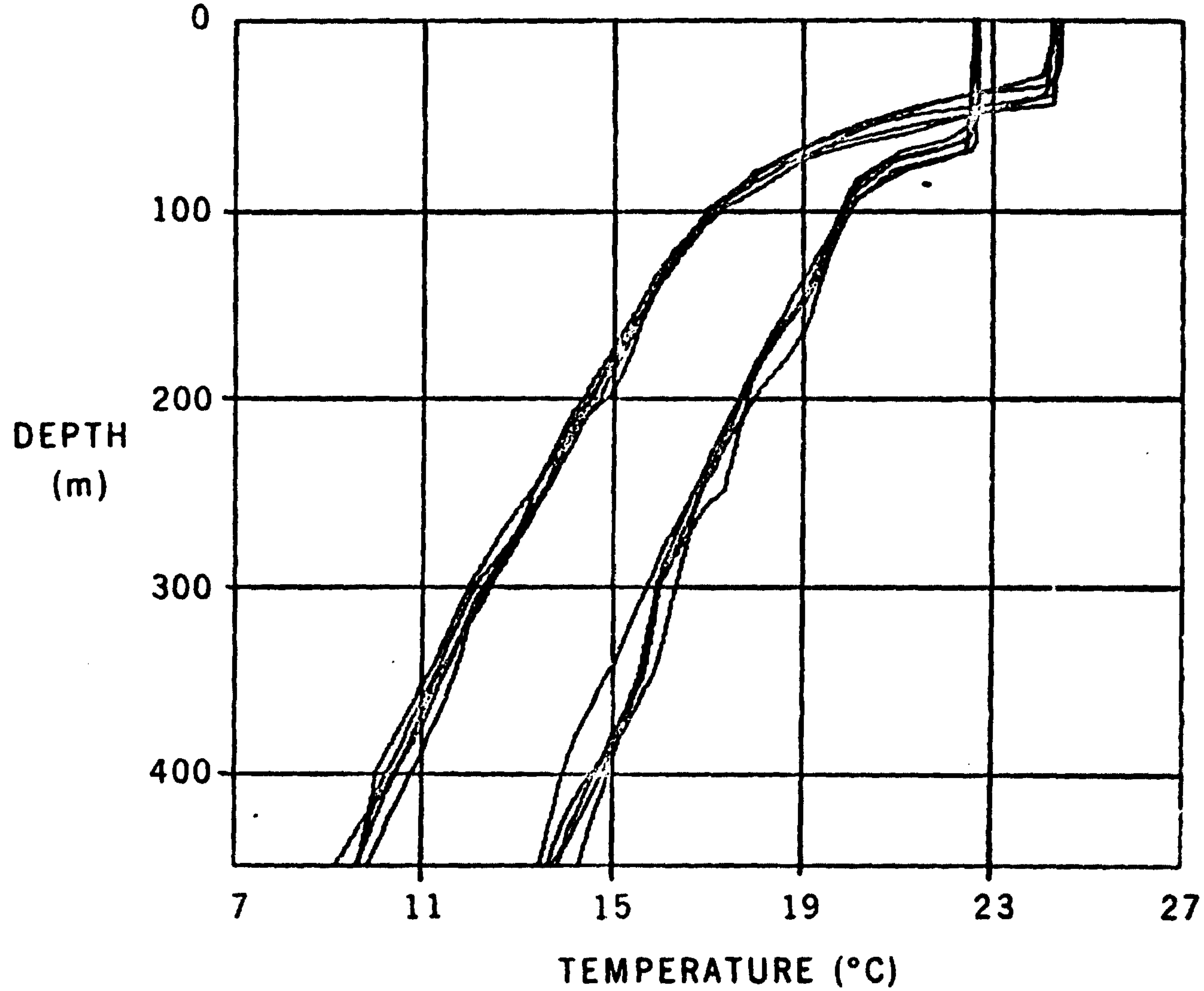

Figure 2c: XBT profiles from a detached warm eddy south of the Tasman Front and a detached cool eddy north of the Front. The warm profiles are from the leg along 36°S in Fig. id between 151.5 and 152.4°E; the cold profiles are from leg HIJ of Fig. 1c, 50km either side of I.

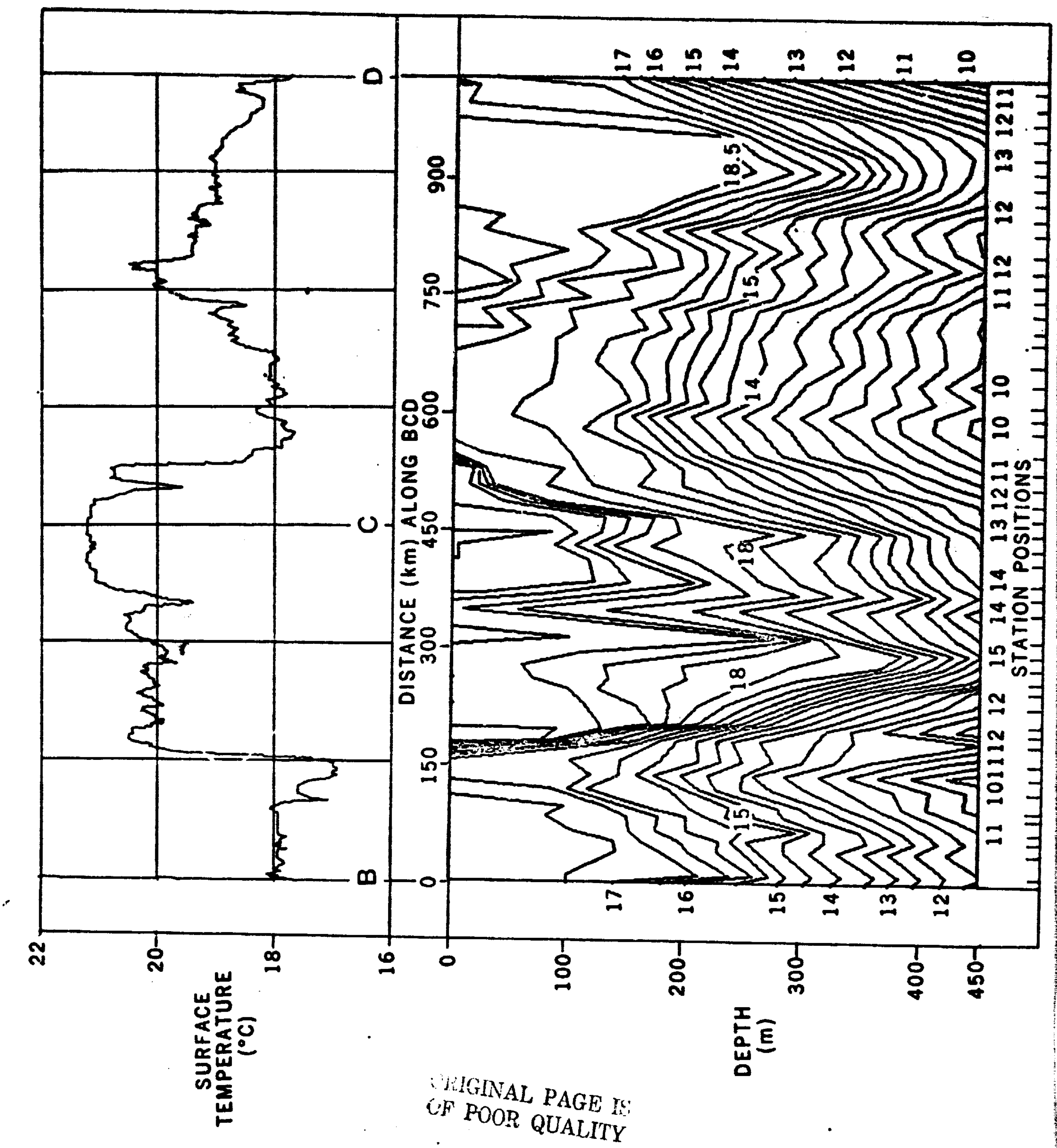

Figure 3a: Vertical isotherm section (°C) from XBT probes and a thermograph sea surface temperature trace along leg BCD of Fig. 1a.

ORIGINAL PAGE IS
OF POOR QUALITY

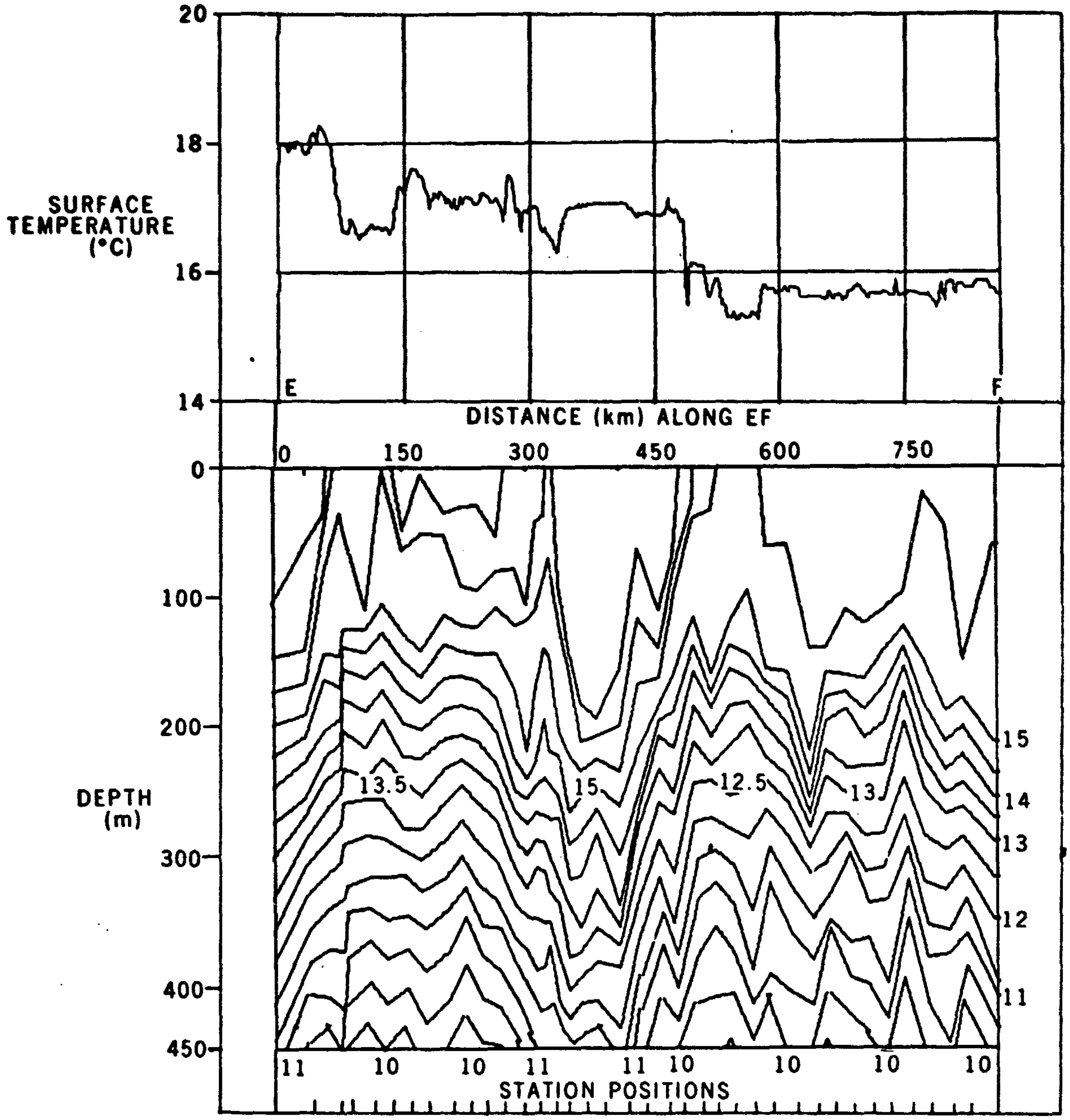

Figure 3b: Vertical isotherm section (^{o}C) from XBT probes and a thermograph sea surface temperature trace along leg EF of Fig. 1a.

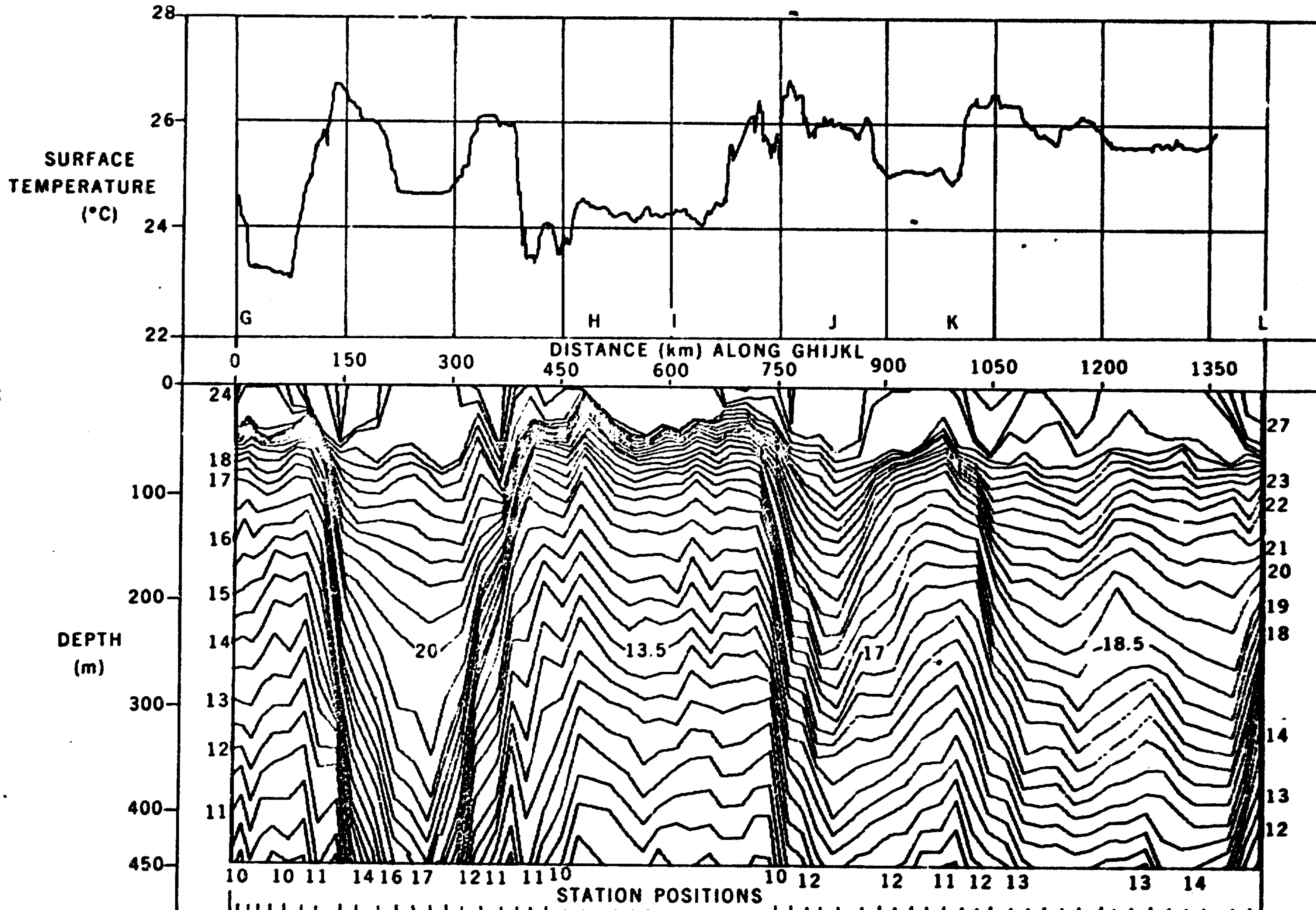

Figure 3c: Vertical isotherm section (^{o}C) from XBT probes and a thermograph sea surface temperature trace along leg GHIJKL of Fig. 1c.

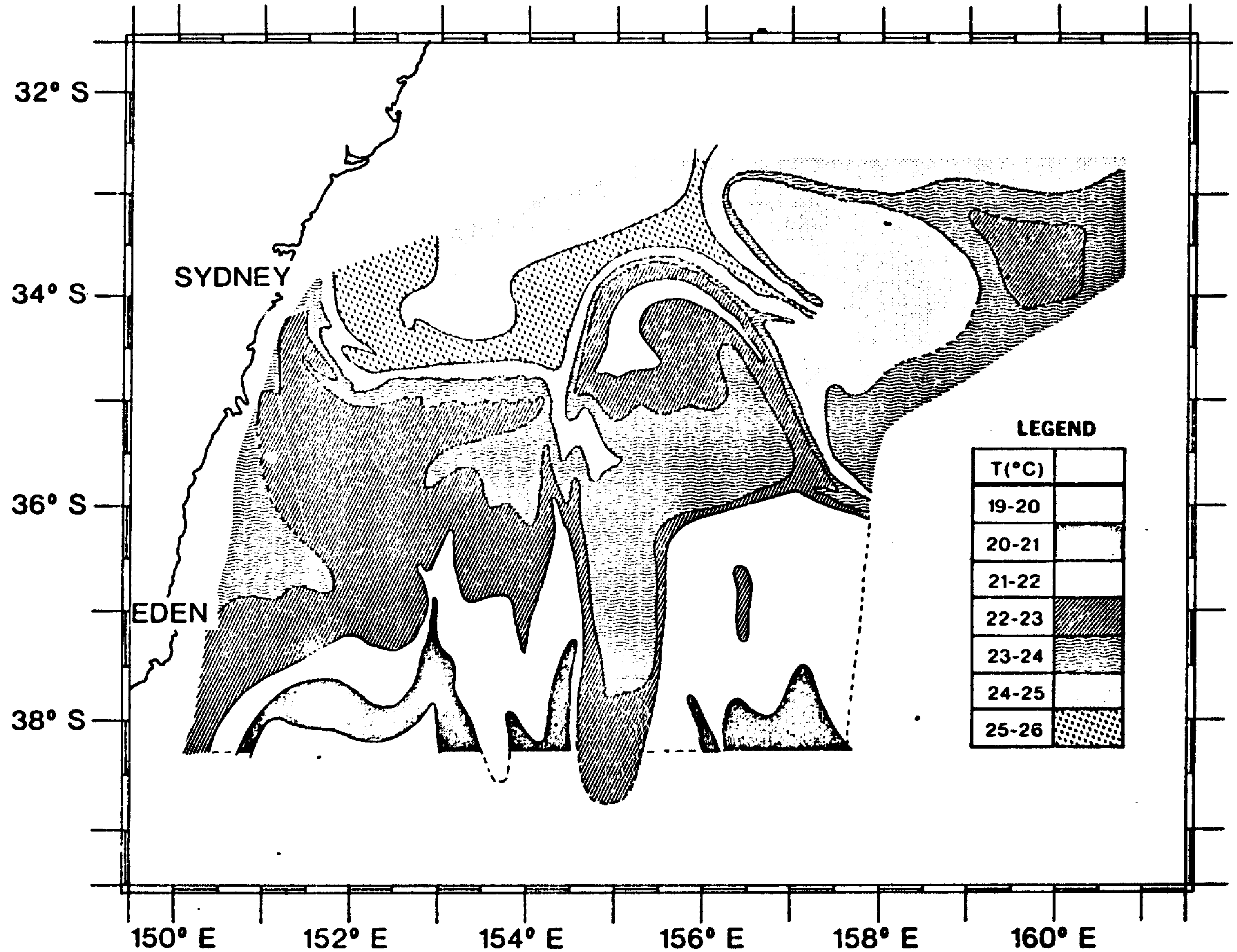

Figure 4: Sea surface temperature patterns from thermograph along cruise track of Fig. 1d. Individual isotherms have been drawn and the regions between have been shaded to show 1°C resolution zones according to the legend.

Figure 5. Digitally enhanced NOAA-4 IR image 13 Oct 77; cold is white.

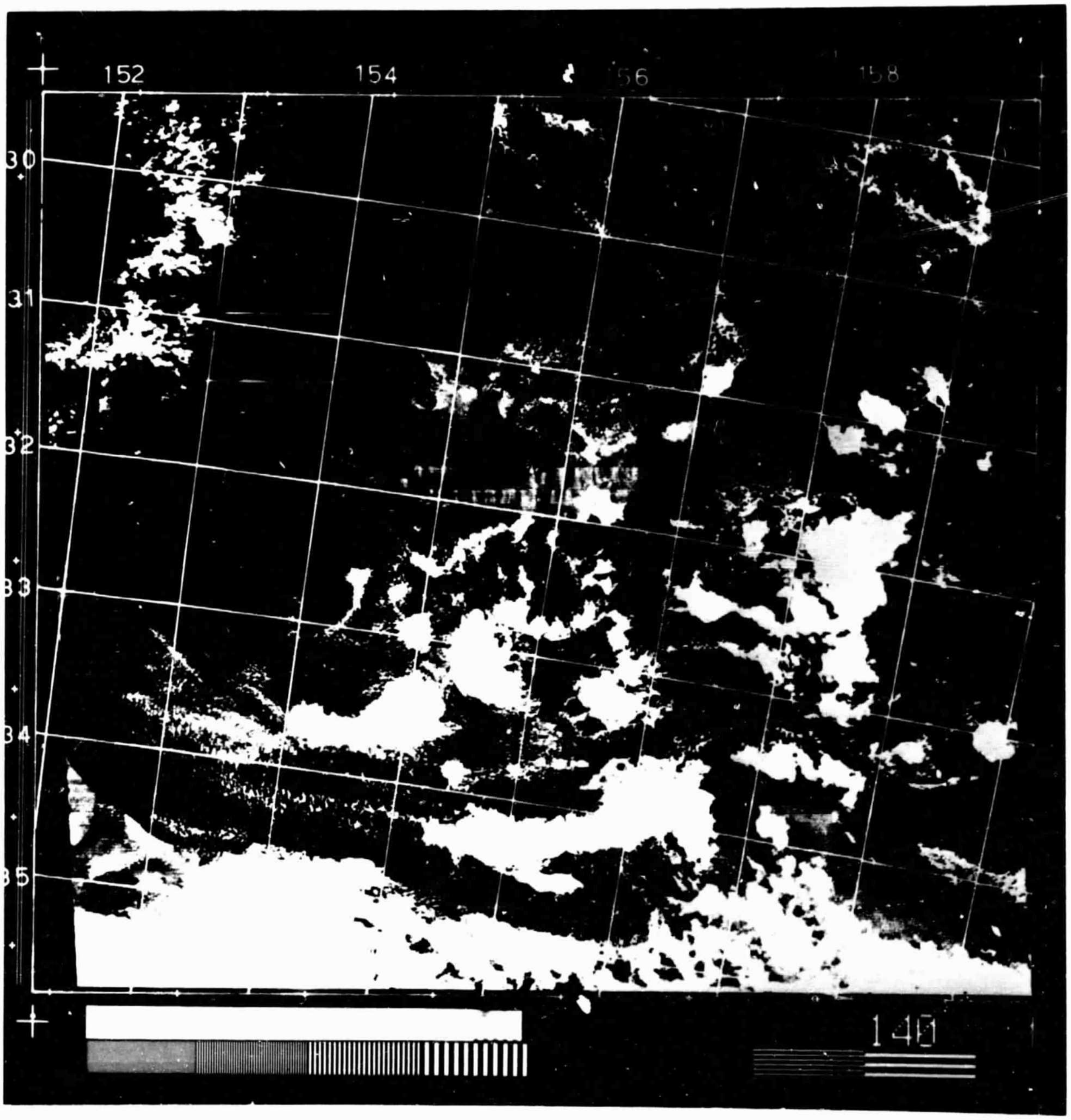

Figure 6. Photographically enhanced HCM IR image 14 Nov 78; cold is white.

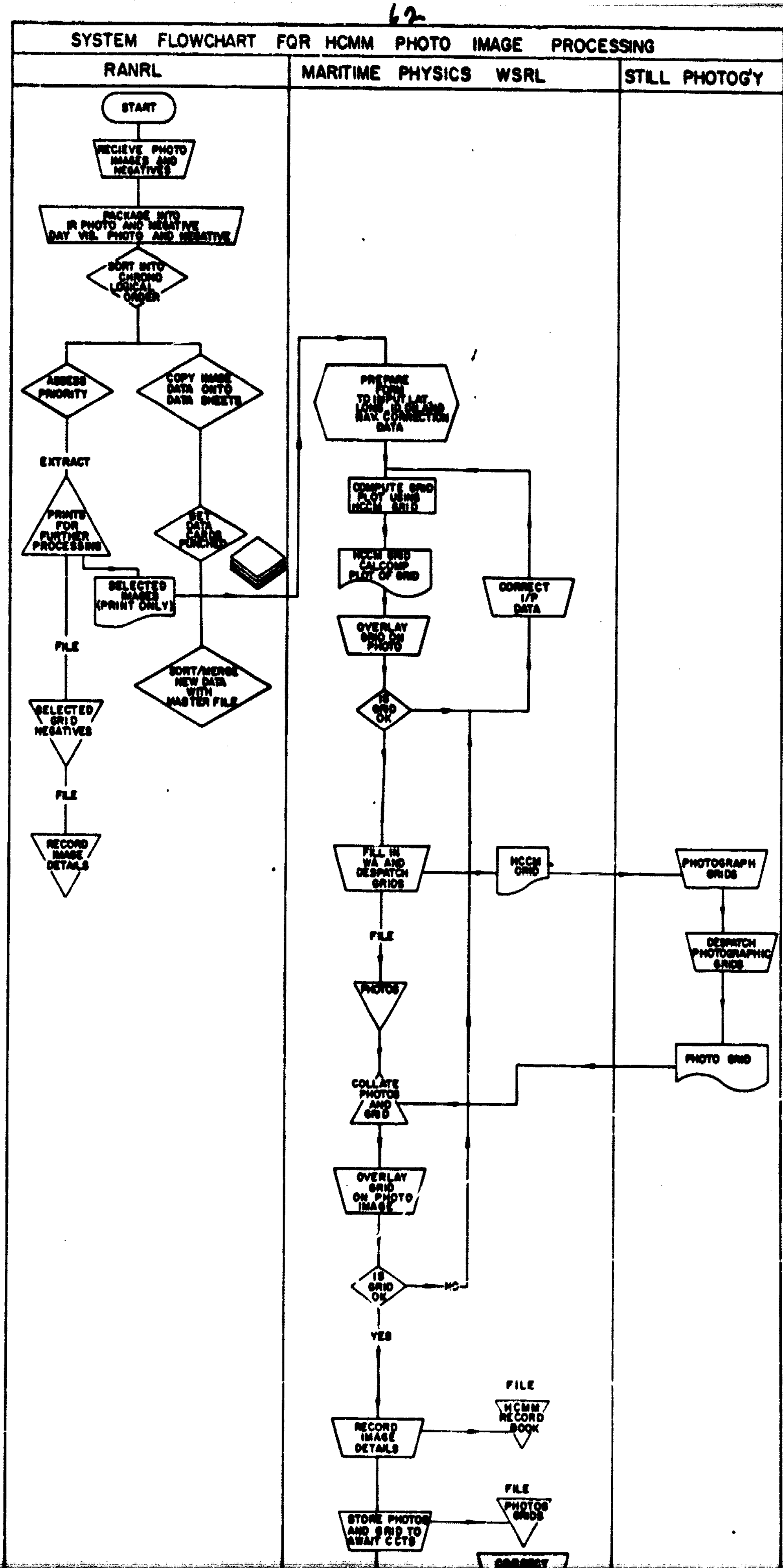

ORIGINAL PAGE IS OF POOR QUALITY

FOLDOUT FRAME

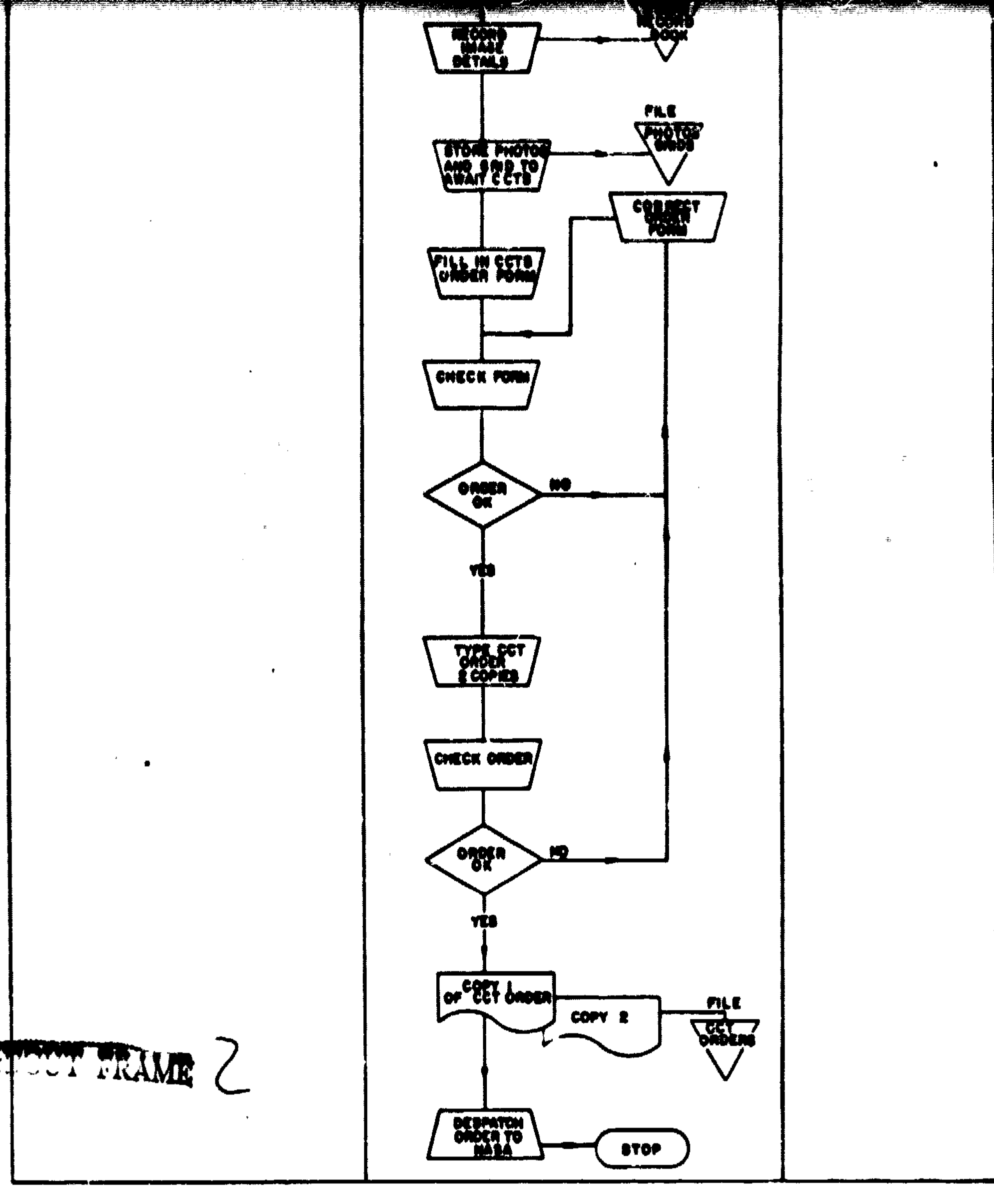

Figure 7. System flowchart for HCM Photo image processing.

63

FOLDOUT FRAME

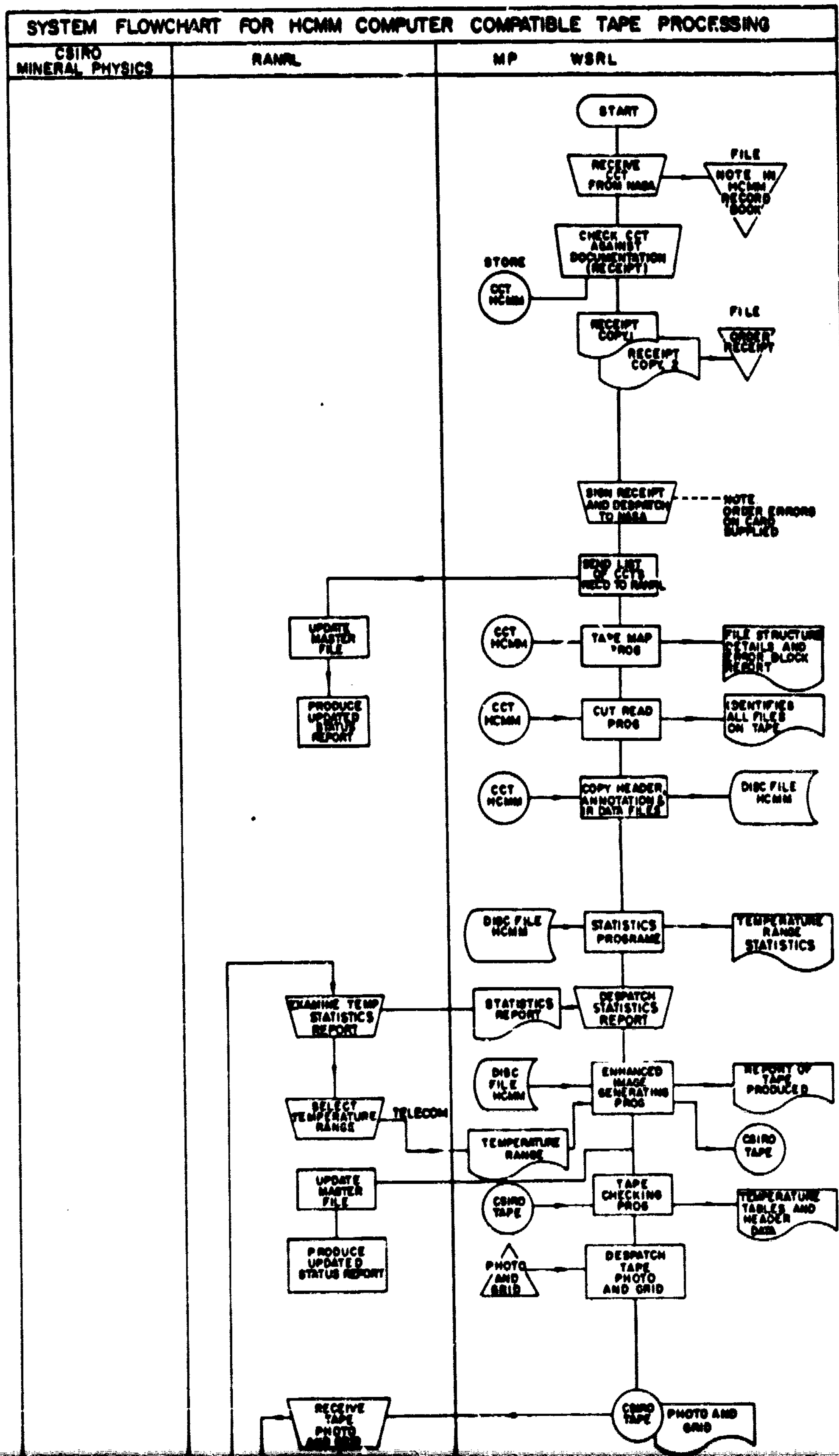

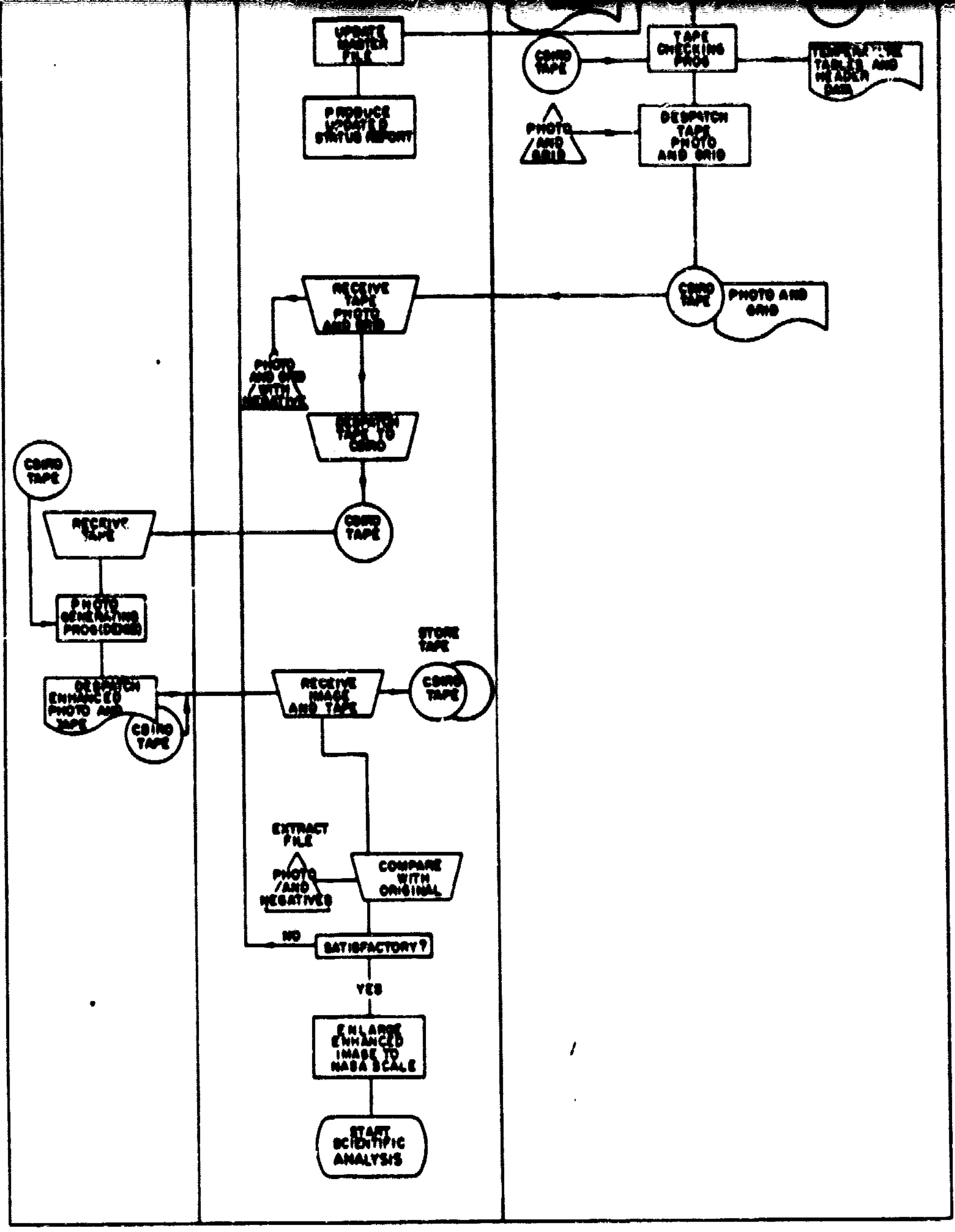

Figure 8. System flowchart for HCM Computer-compatible Tape(CCT) processing.

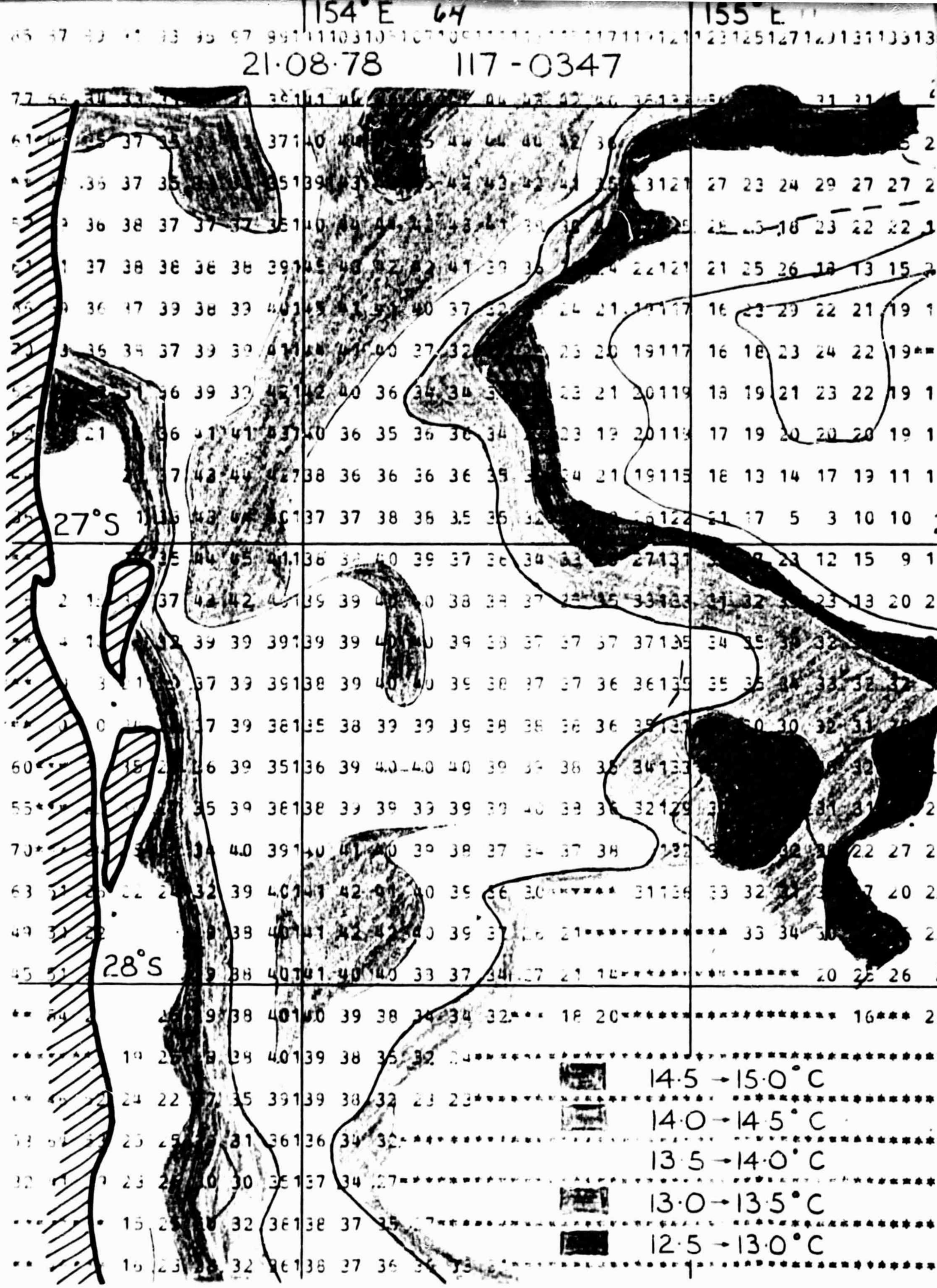

Figure 9. Contoured output of the "statistics" program for image 117-03470-2. This program derives mean temperatures for each 20 X 20 pixel box of the CCT image data. Each such box is 2mm square on the photo-images (Figs. 11 and 12).

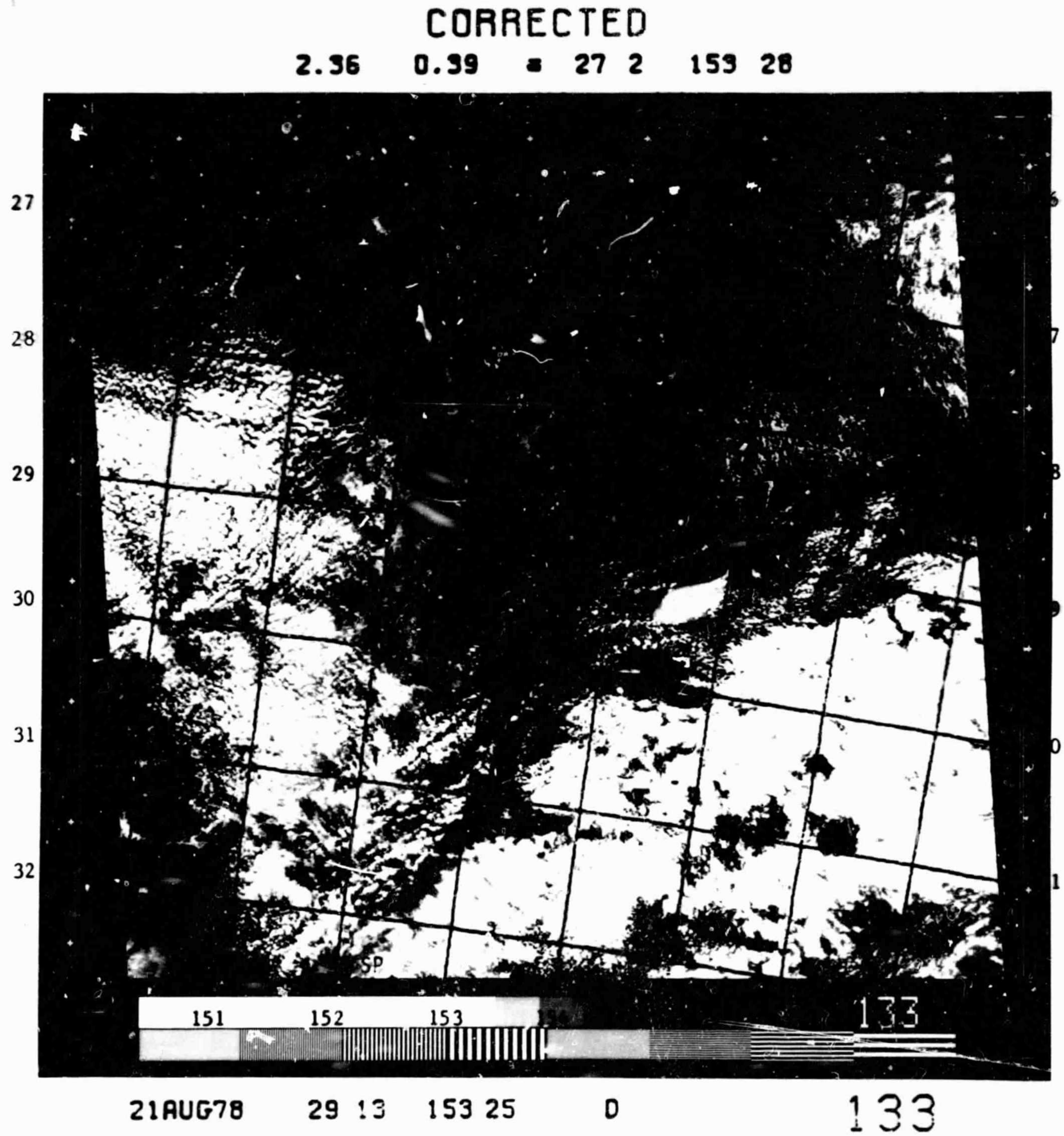

Figure 11. Standard NASA HCM IR image 21 Aug 78 (daytime); cold is white.

Fig. 10. Corrected cordinate grid overlay for HCM image 117-03470-2 (Fig. 11)

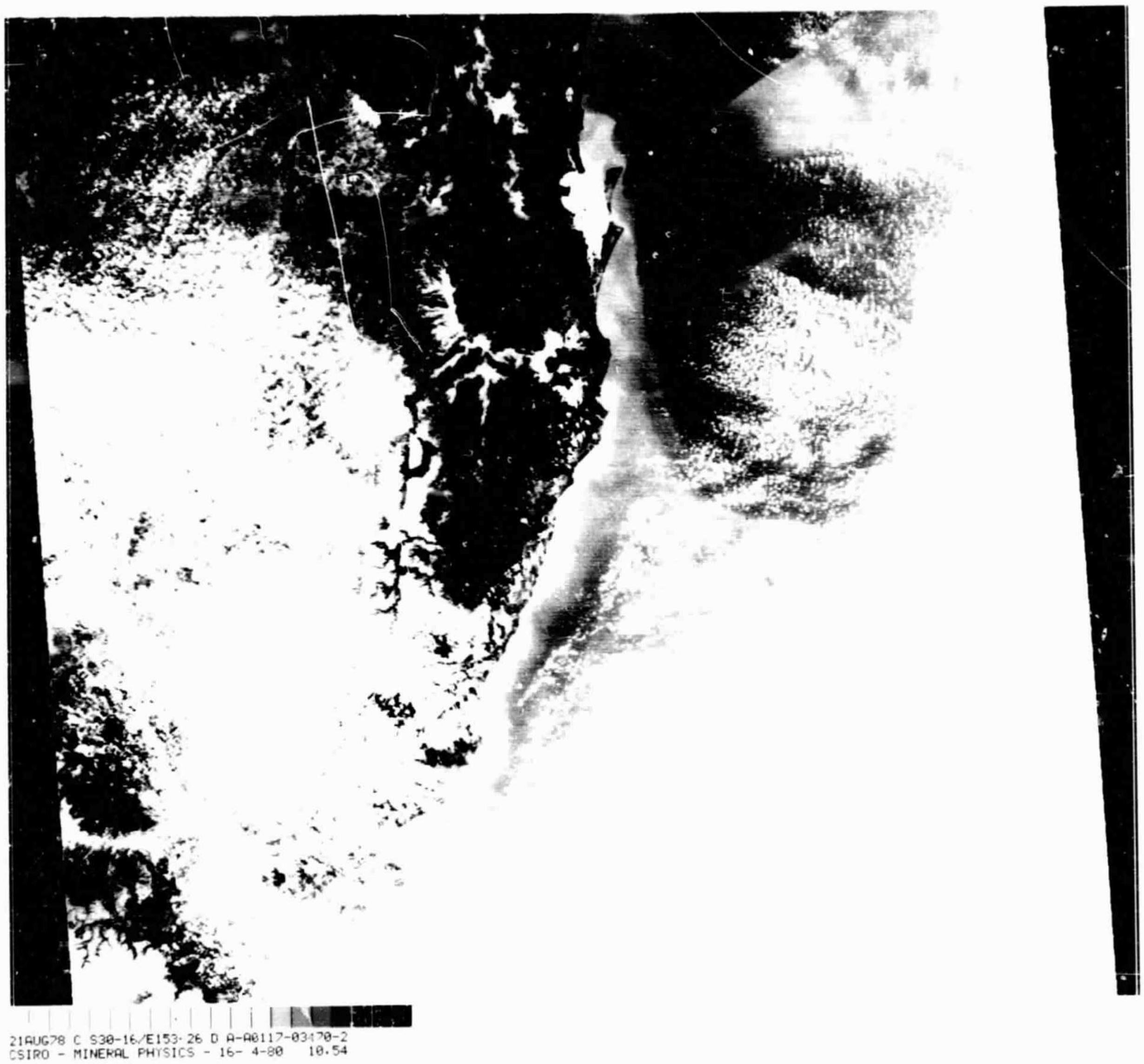

Figure 12. Digitally enhanced HCM IR image from CCT data for 21 Aug 78 (daytime); cold is white.

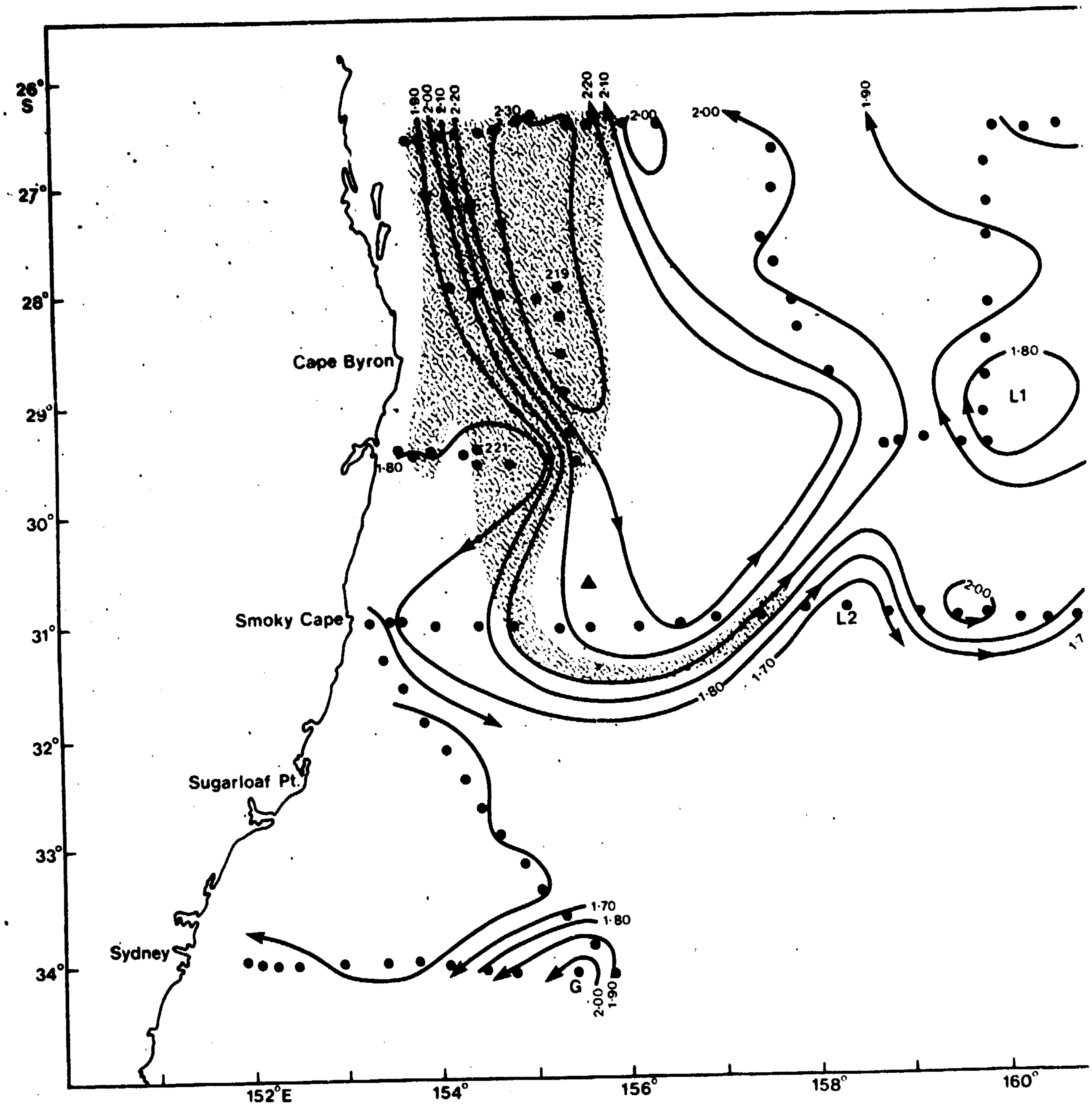

Figure 13. Surface dynamic topography (dyn m re 1300 dbar) for CSIRO Cruise SP 11/78 (5-18 Aug 78). The warm core is shown by the stippled area; courtesy F.M.Boland and J.A.Church, CSIRO.